Electronic Supplementary Information

For

Strategically Designed Biomodel: Engineering C3-C4 Cleavage of D-Fructose

Palwinder Singh*, Arun Kumar, Sukhmeet Kaur, Amrinder Singh

Centre for Advanced Studies, Department of Chemistry, Guru Nanak Dev University, Amritsar-143005. India

Table of contents

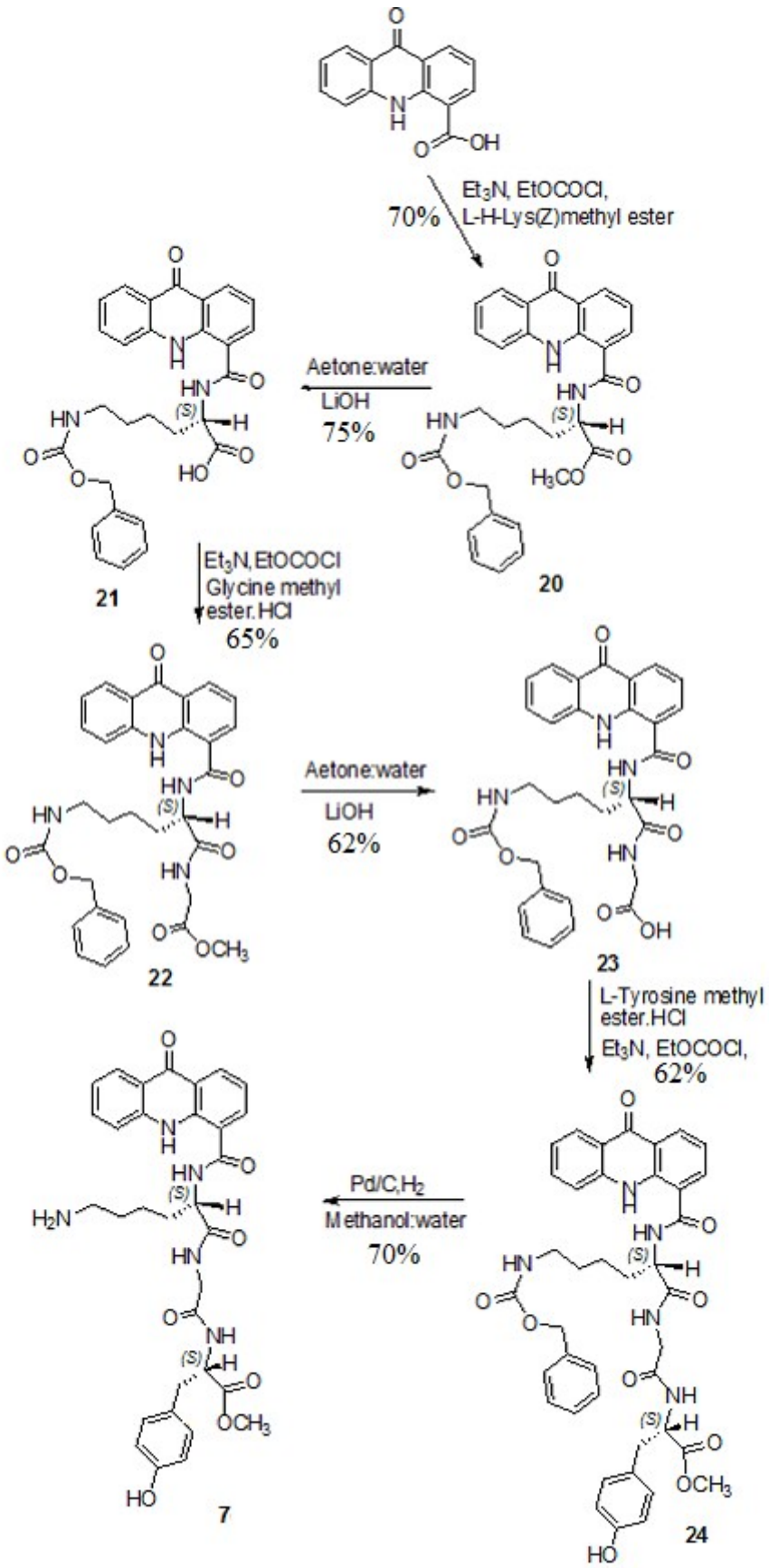

Scheme S1. Synthesis of compound **7**.

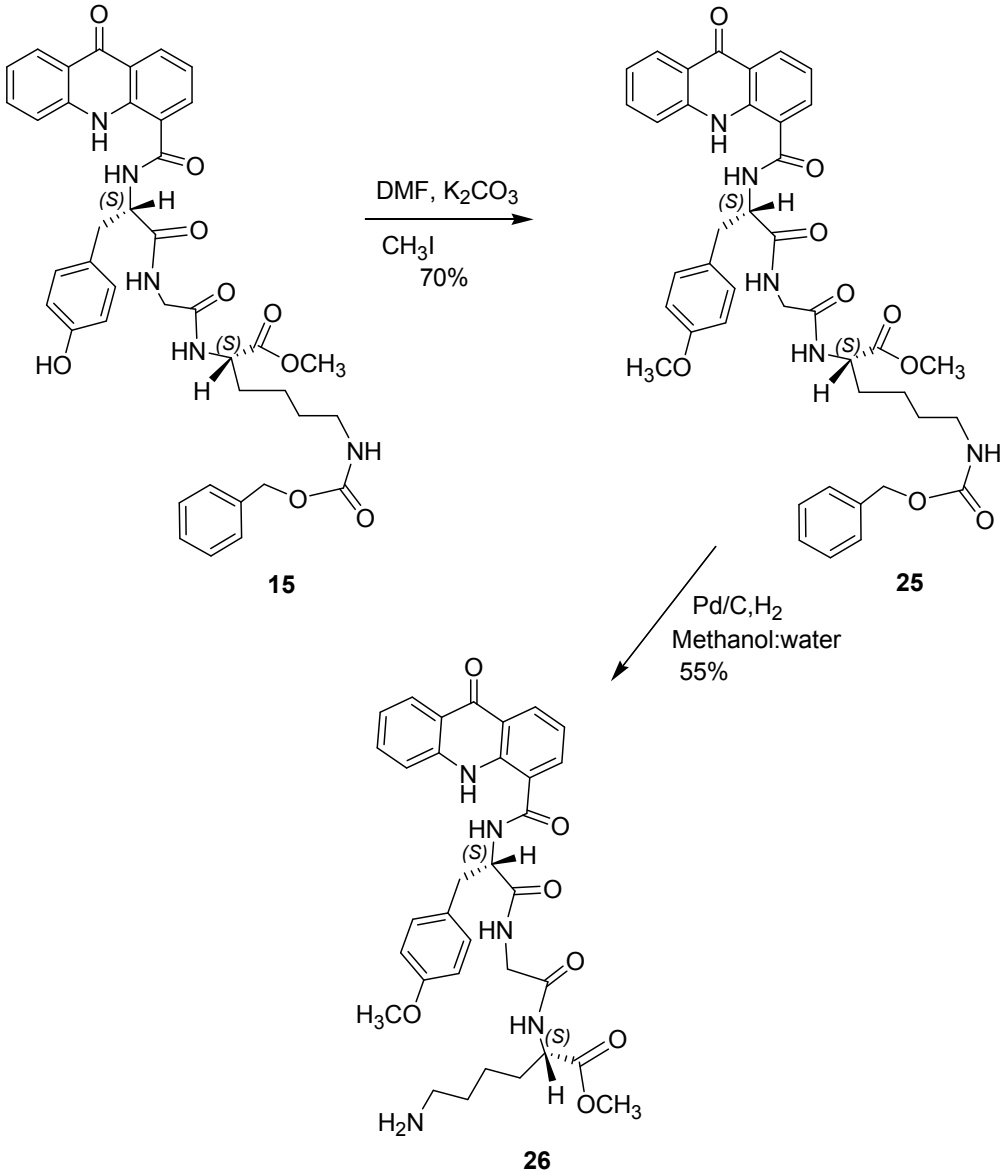

Scheme S2

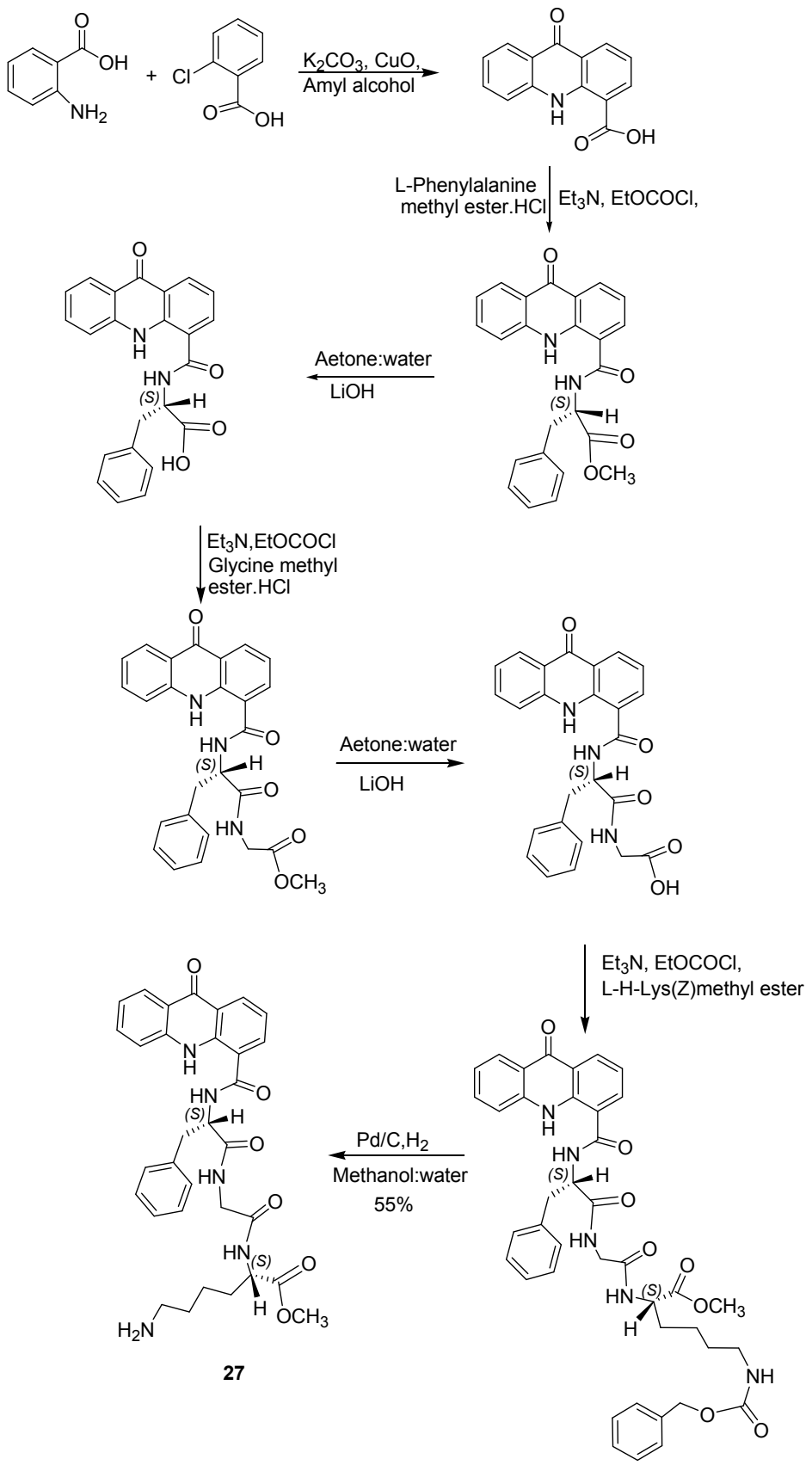
K2CO3, CuO,
Amyl alcohol
L-Phenylalanine methyl ester.HCl
Et3N, EtOCOCl,
Aetone:water
LiOH
Et3N,EtOCOCl
Glycine methyl ester.HCl
Aetone:water
LiOH
Et3N, EtOCOCl,
L-H-Lys(Z)methyl ester
Pd/C,H2
Methanol:water
55%
27

Scheme S3

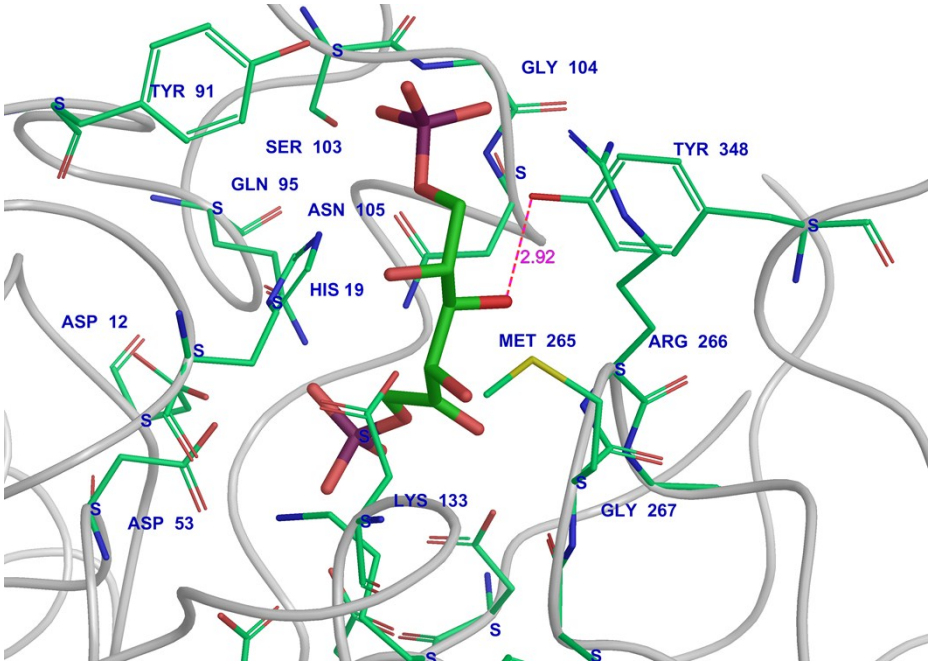

Figure S1. Crystal coordinates of aldolase in association with fructose-bisphosphate (pdb ID 1umg)[6e]. All amino acids have *S*-configuration at C_{α}. C4-OH of fructose is close to (2.92 Å) phenolic group of Tyr. Hs′ are omitted for clarity.

LC-MS of compounds 4-7. Procedure for recording LC-MS is mentioned in the General note.

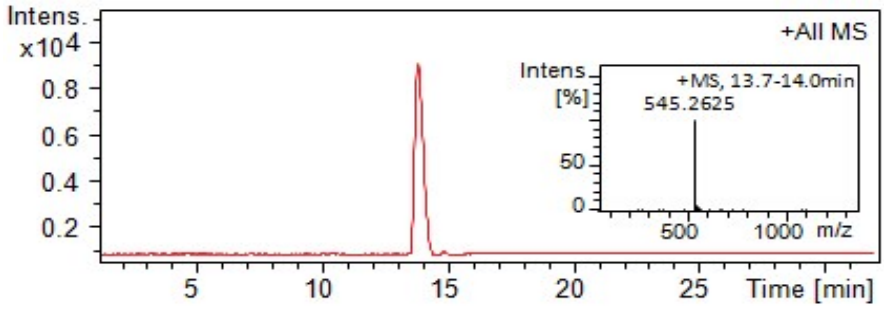

Figure S2. LC-MS of compound **4a**.

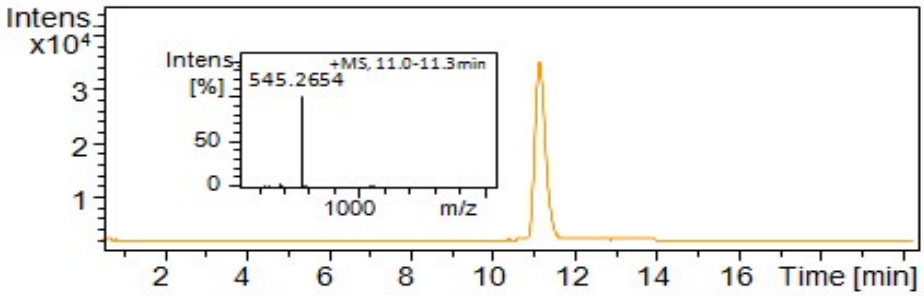

Figure S3. LC-MS of compound **4b**.

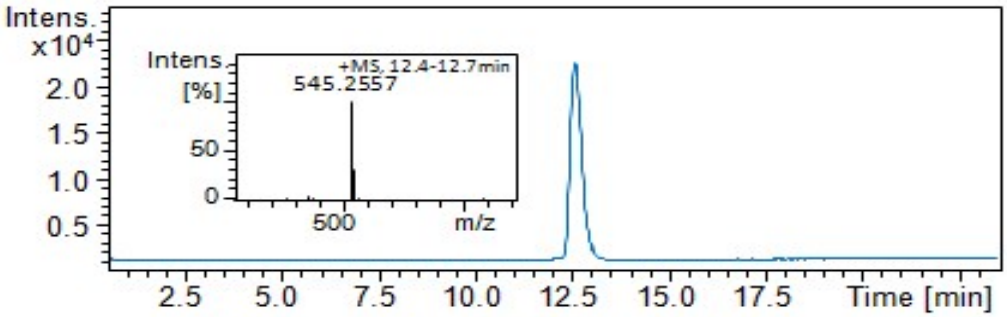

Figure S4. LC-MS of compound **4c**.

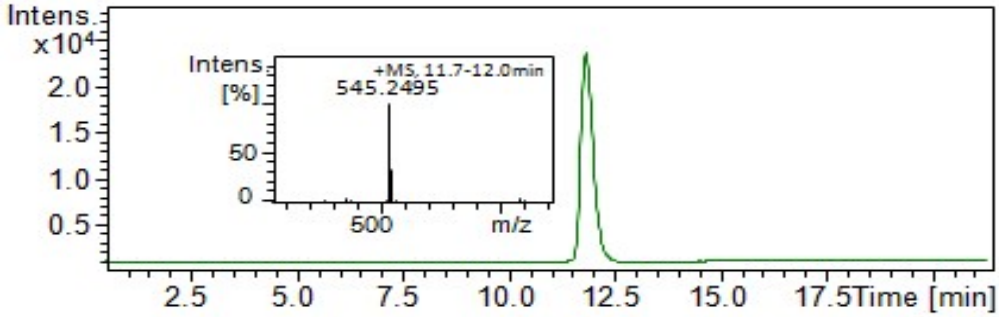

Figure S5. LC-MS of compound **4d**.

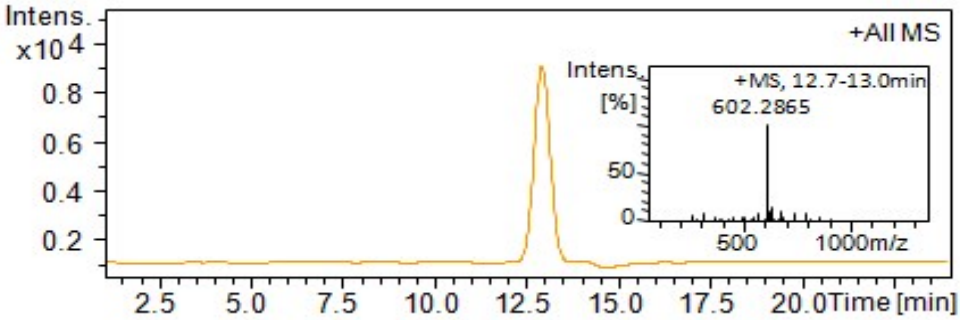

Figure S6. LC-MS of compound **5a**.

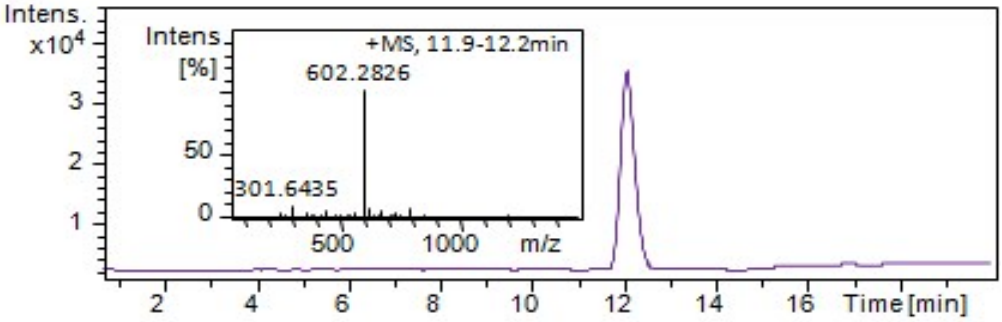

Figure S7. LC-MS of compound **5b**.

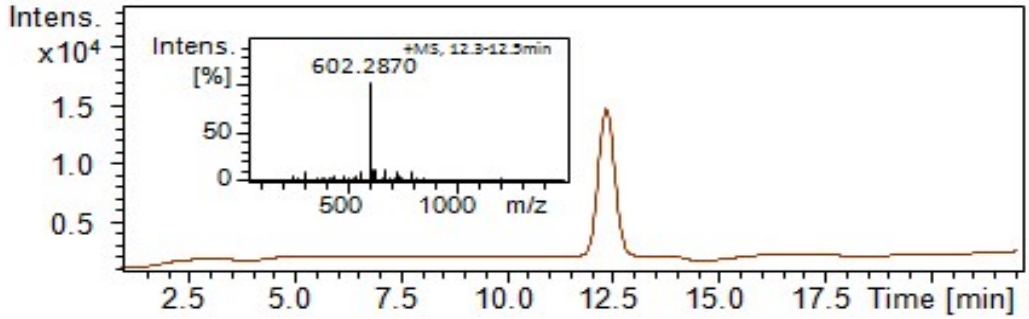

Figure S8. LC-MS of compound **5c**.

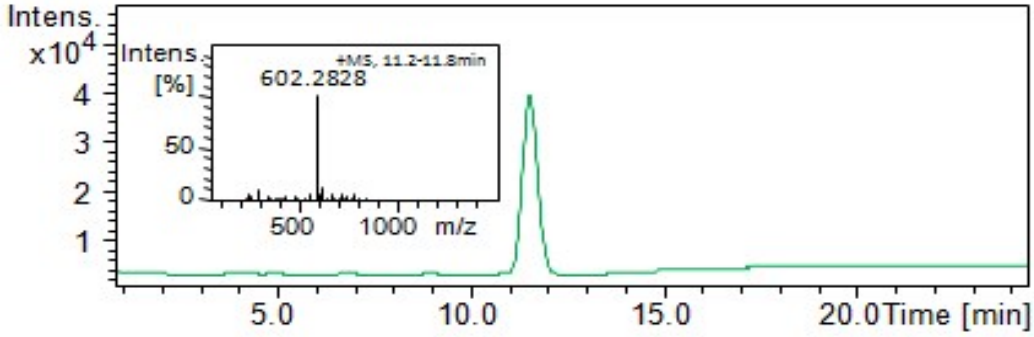

Figure S9. LC-MS of compound **5d**.

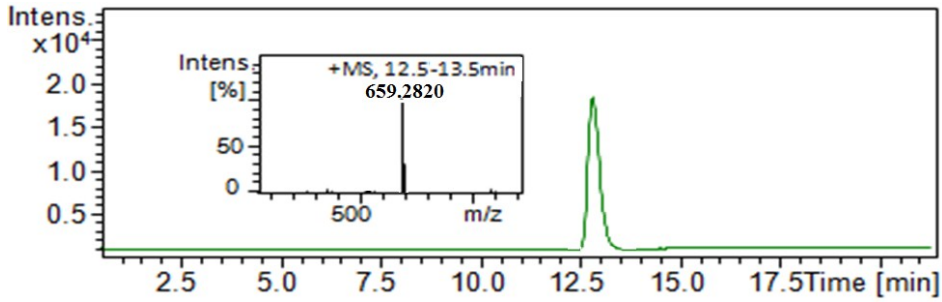

Figure S10. LC-MS of compound **6a**.

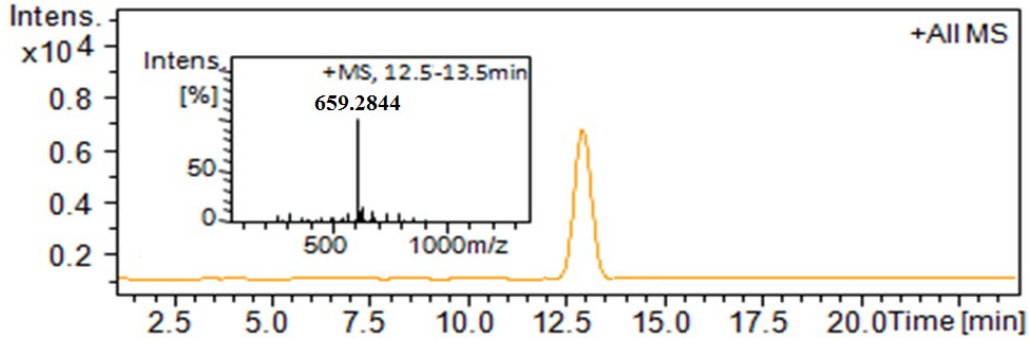

Figure S11. LC-MS of compound **6b**.

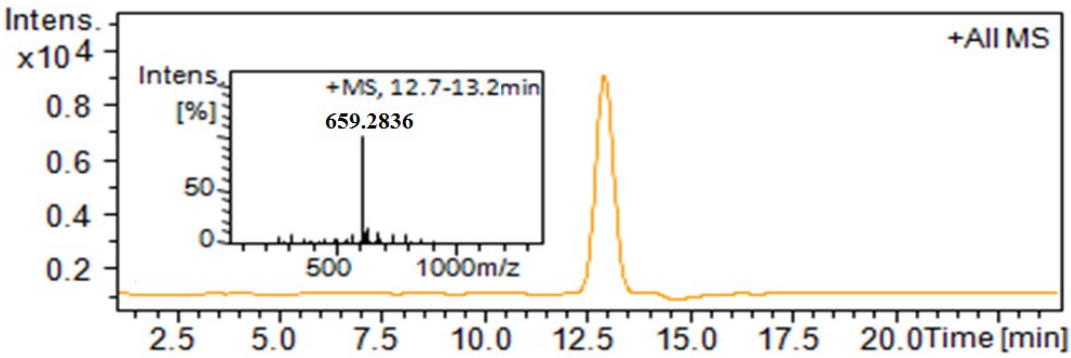

Figure S12. LC-MS of compound **6c**.

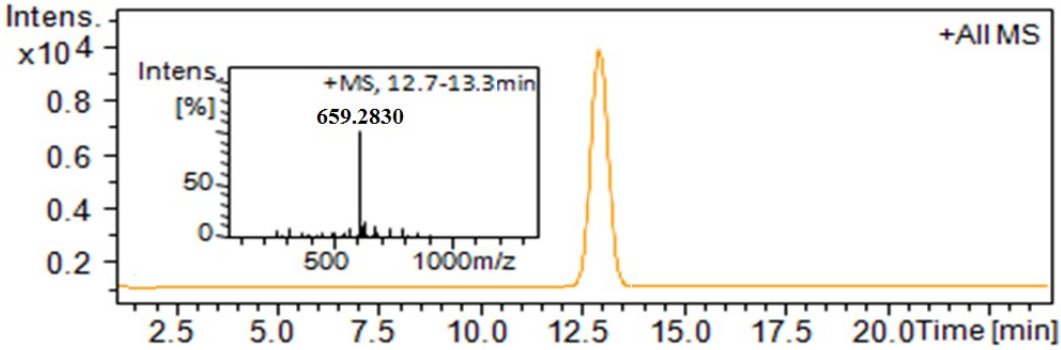

Figure S13. LC-MS of compound **6d**.

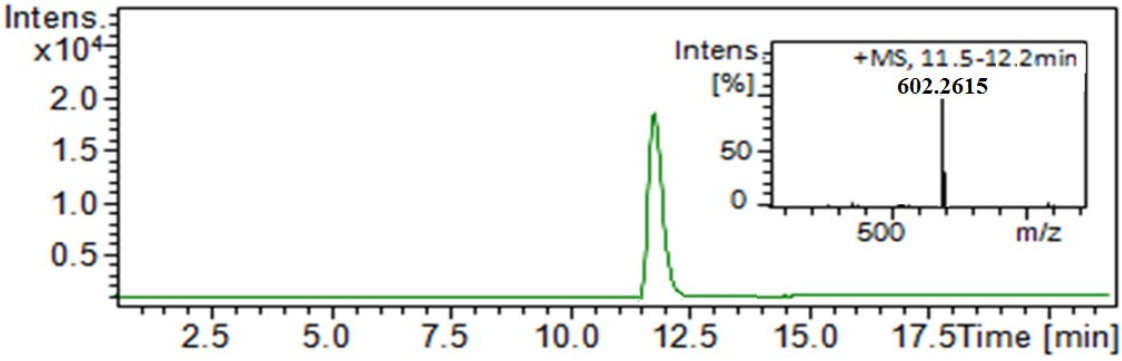

Figure S14. LC-MS of compound **7**.

NMR Spectra

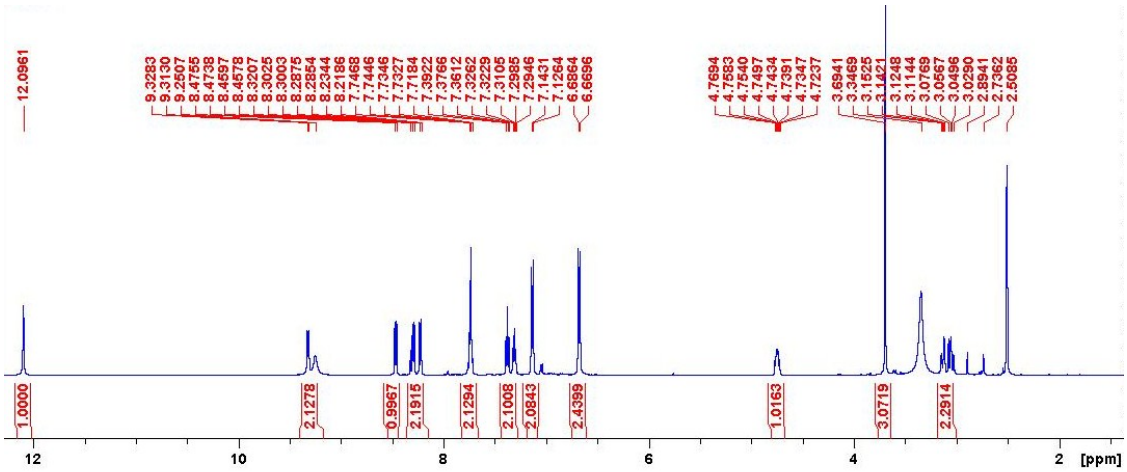

Figure S15. ^{1}H NMR spectrum of compound **11**.

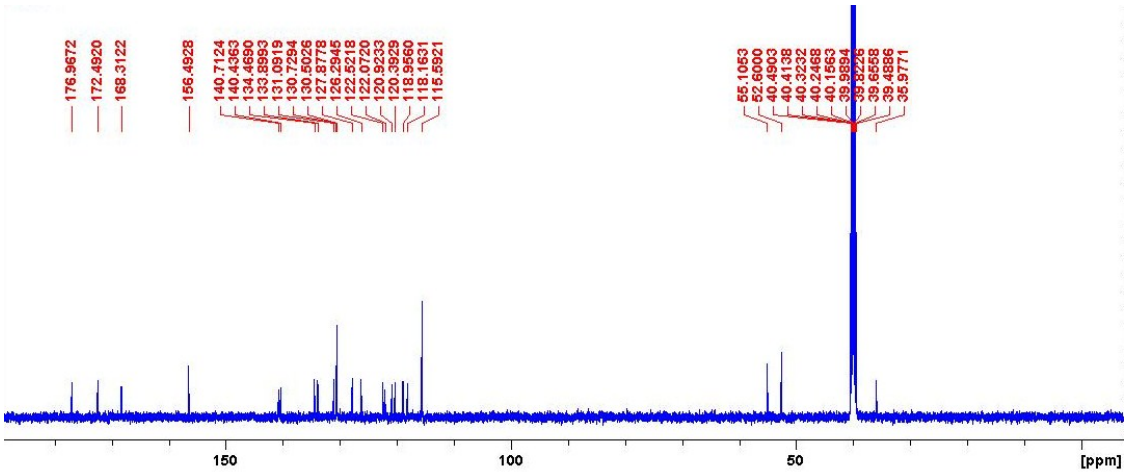

Figure S16. ^{13}C NMR spectrum of compound **11**.

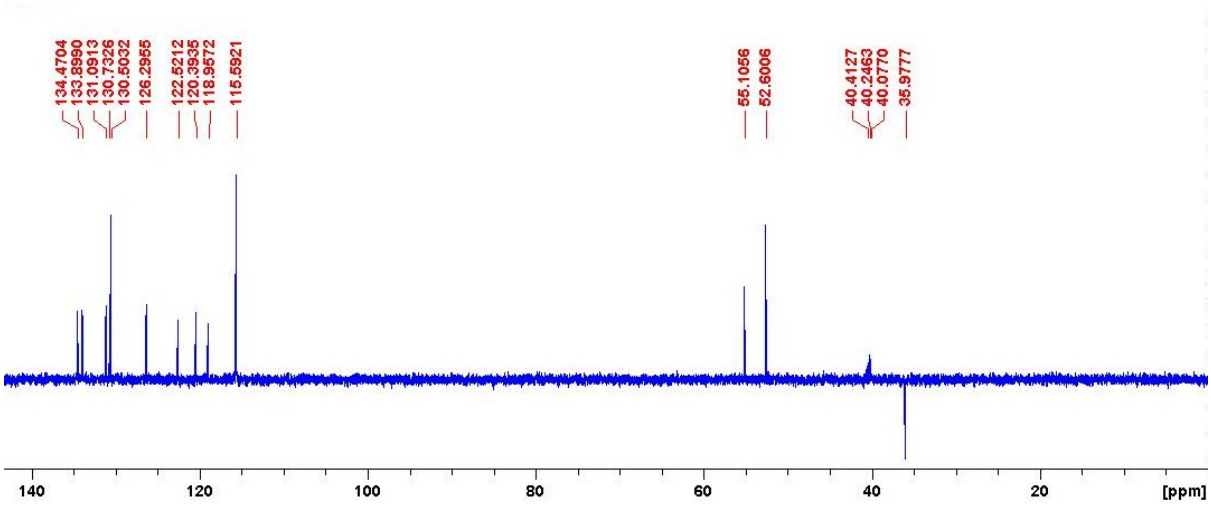

Figure S17. DEPT-135 NMR spectrum of compound **11**.

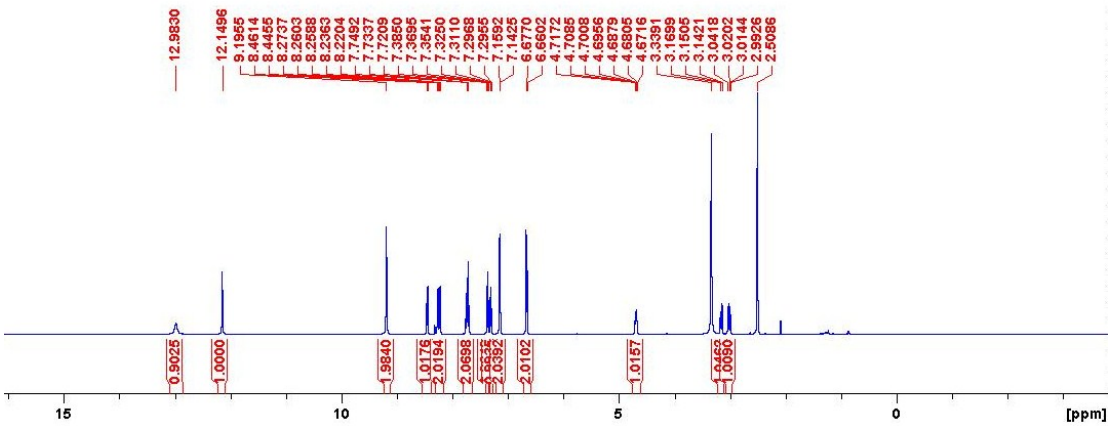

Figure S18. ^{1}H NMR spectrum of compound **12**.

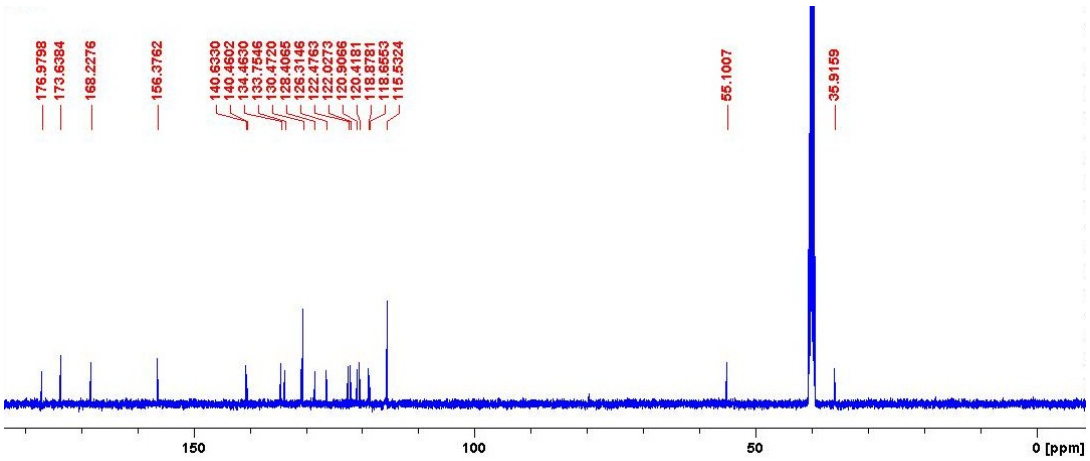

Figure S19. ^{13}C NMR spectrum of compound **12**.

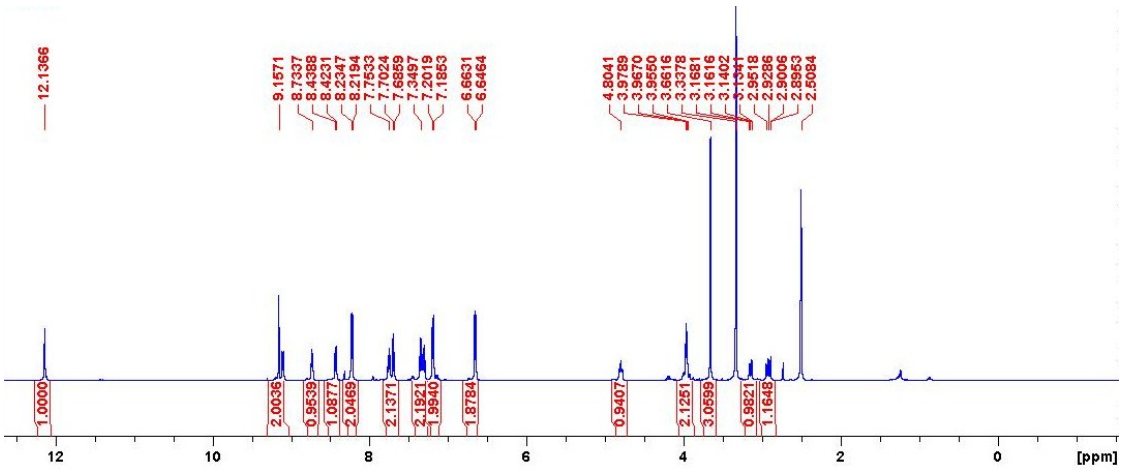

Figure S20. ^{1}H NMR spectrum of compound **13**.

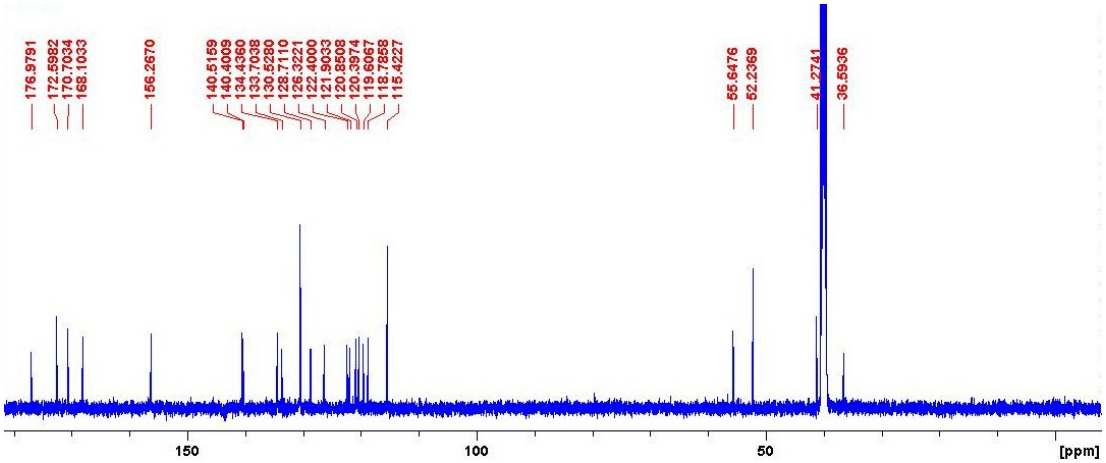

Figure S21. ^{13}C NMR spectrum of compound **13**.

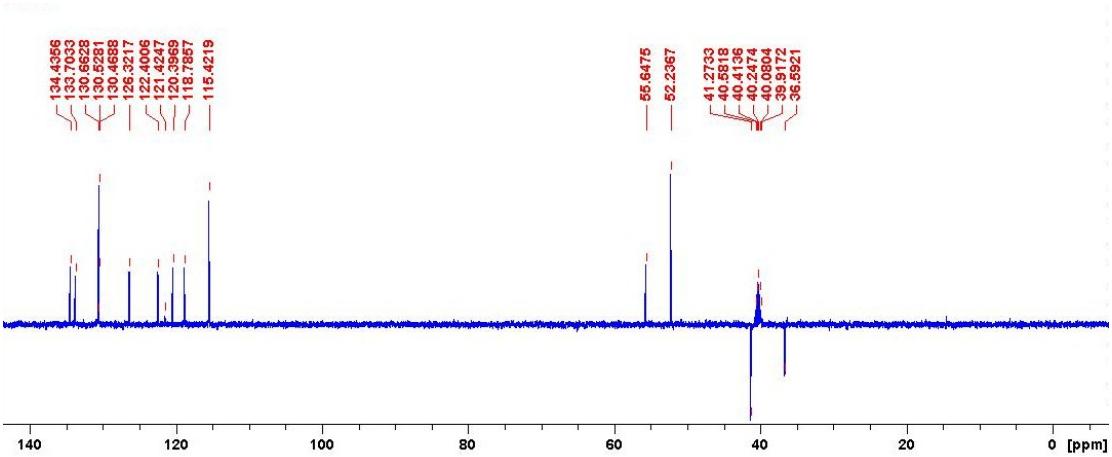

Figure S22. DEPT-135 NMR spectrum of compound **13**.

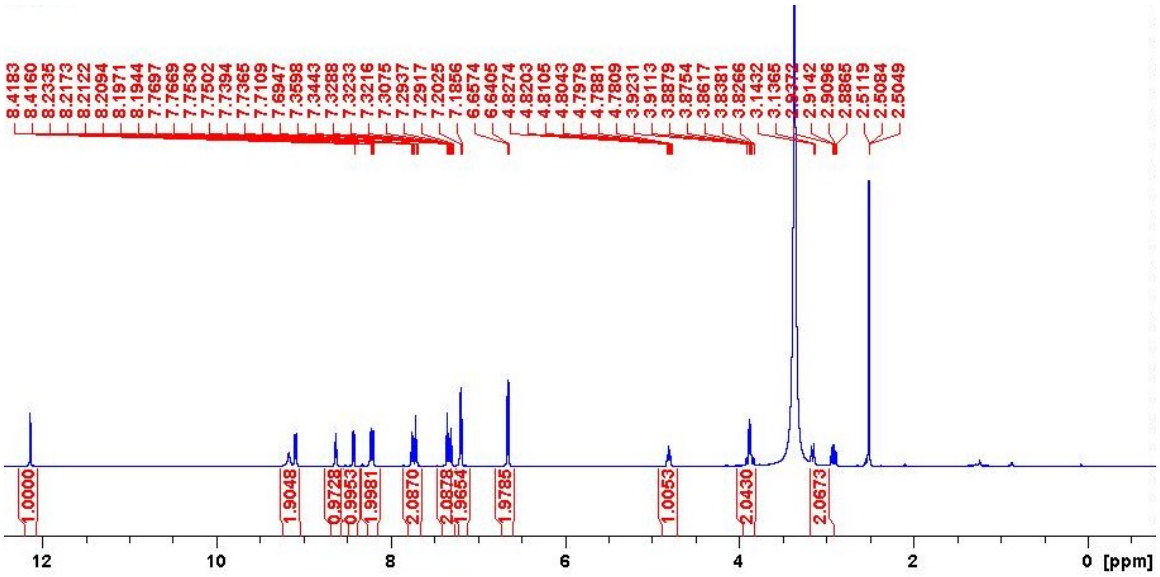

Figure S23. ^{1}H NMR spectrum of compound **14**.

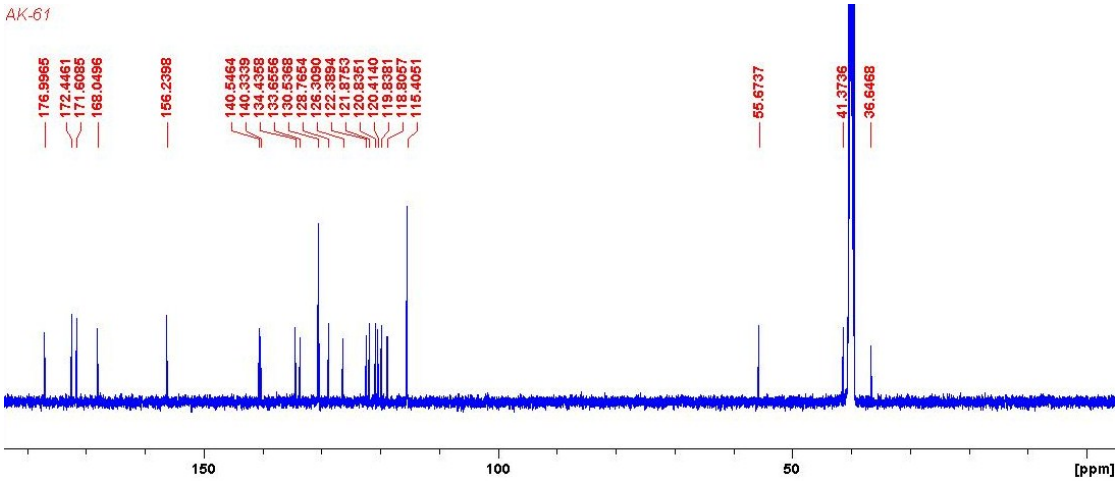

Figure S24. ^{13}C NMR spectrum of compound **14**.

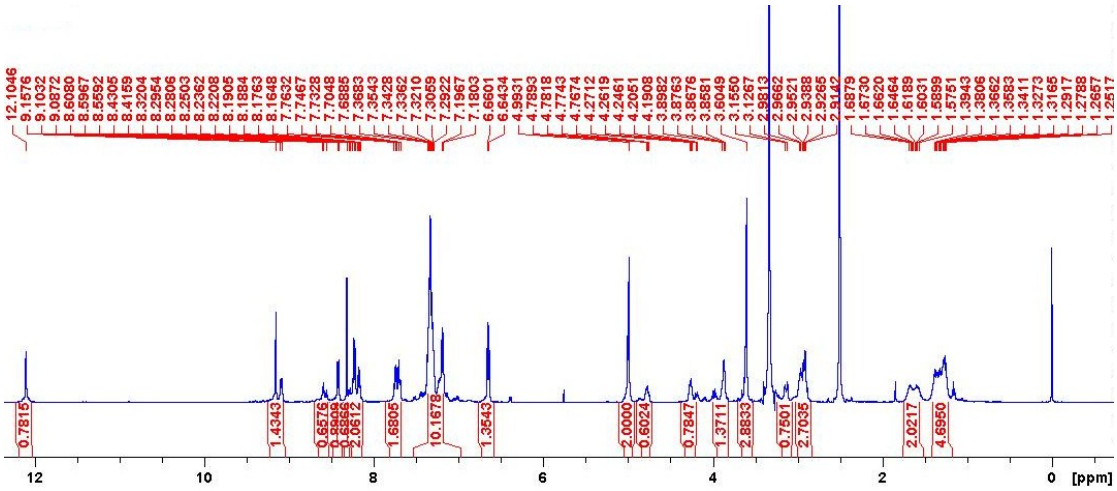

Figure S25. ^{1}H NMR spectrum of compound **15**.

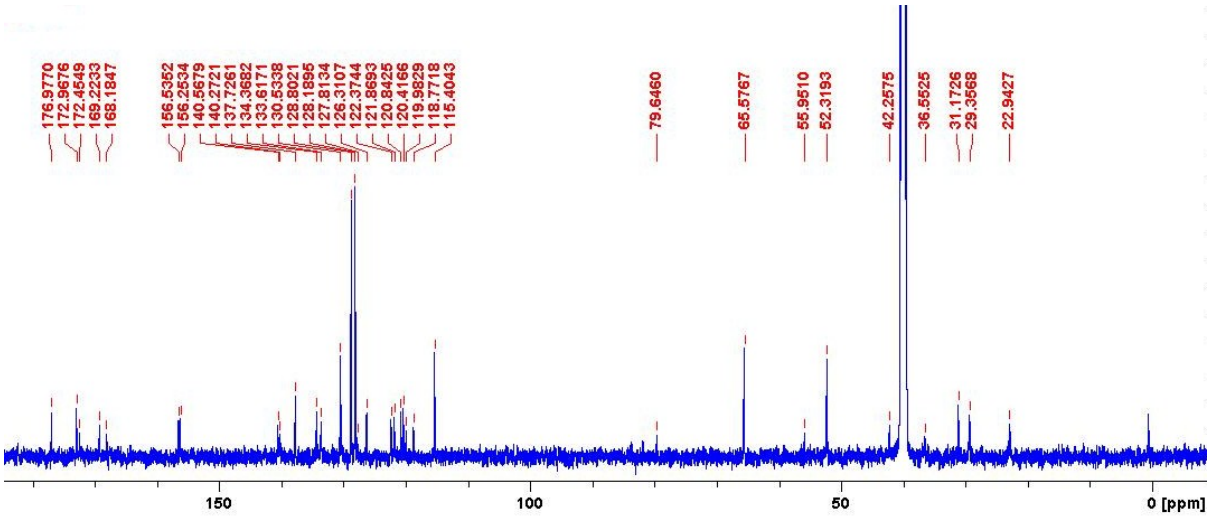

Figure S26. ^{13}C NMR spectrum of compound **15**.

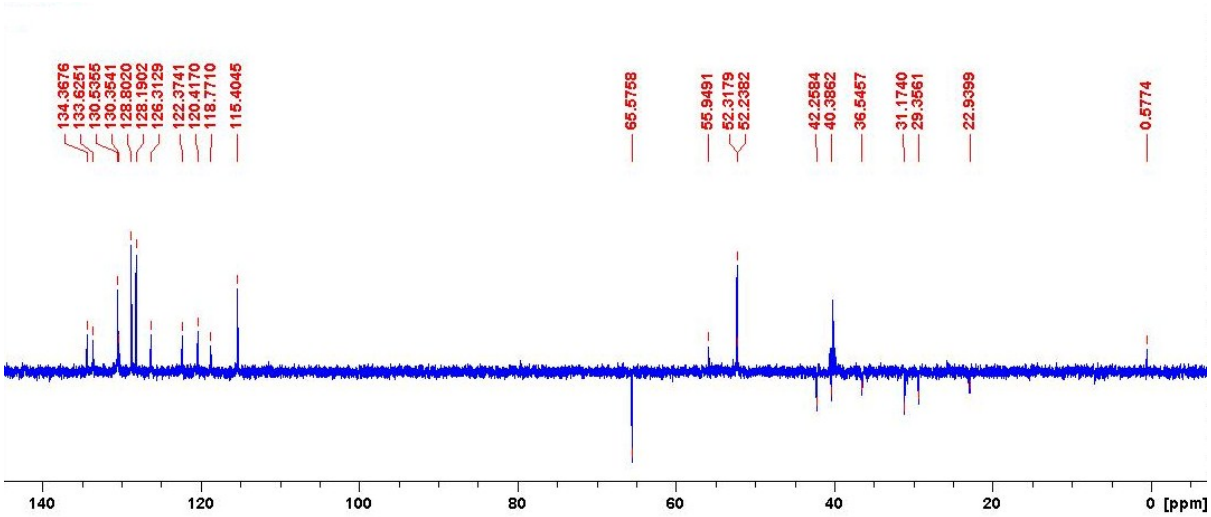

Figure S27. DEPT-135 NMR spectrum of compound **15**.

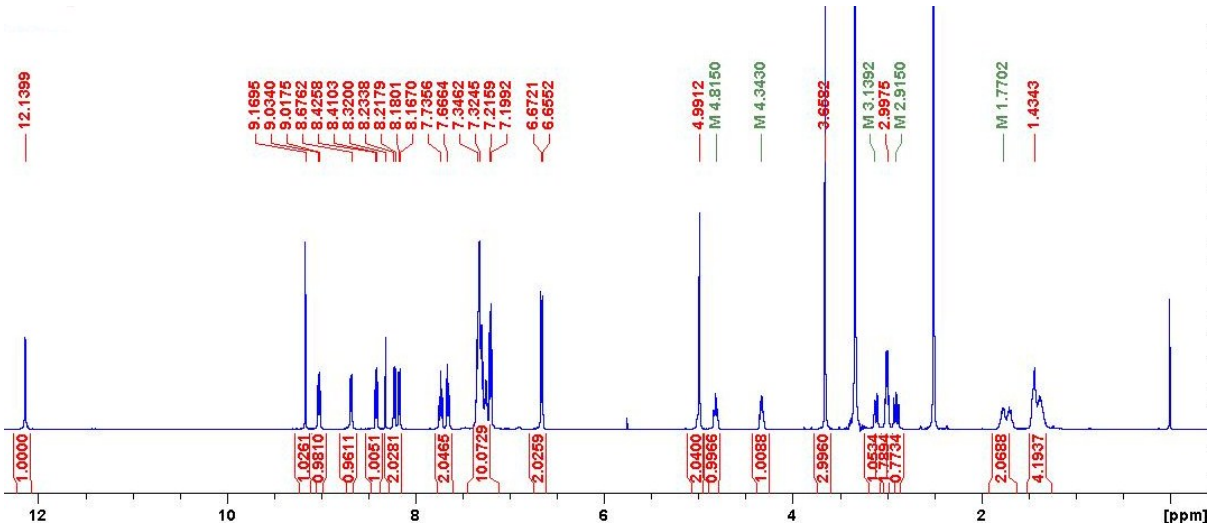

Figure S28. ^{1}H NMR spectrum of compound **16**.

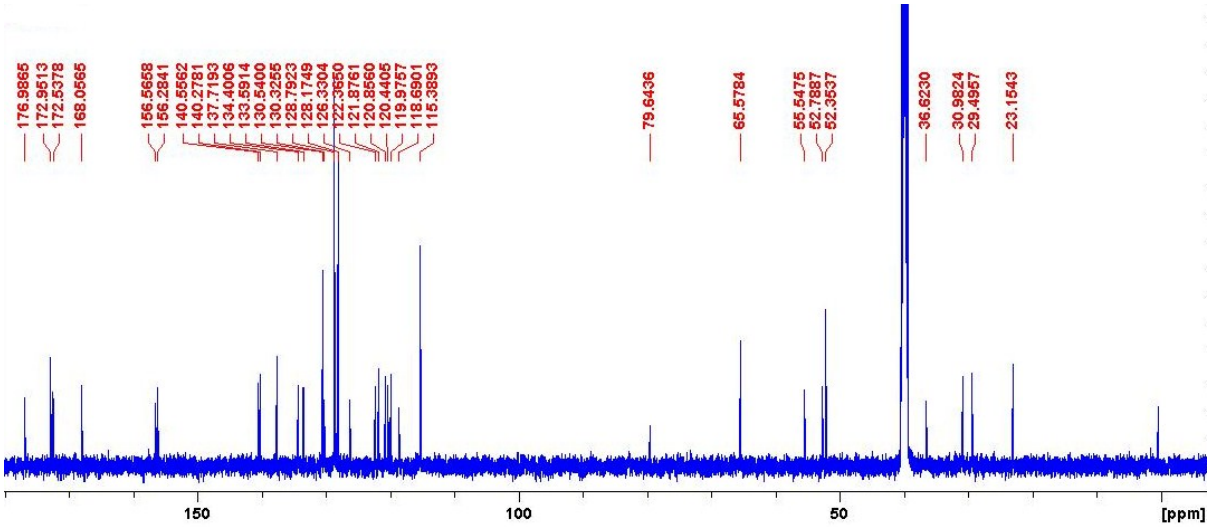

Figure S29. ^{13}C NMR spectrum of compound **16**.

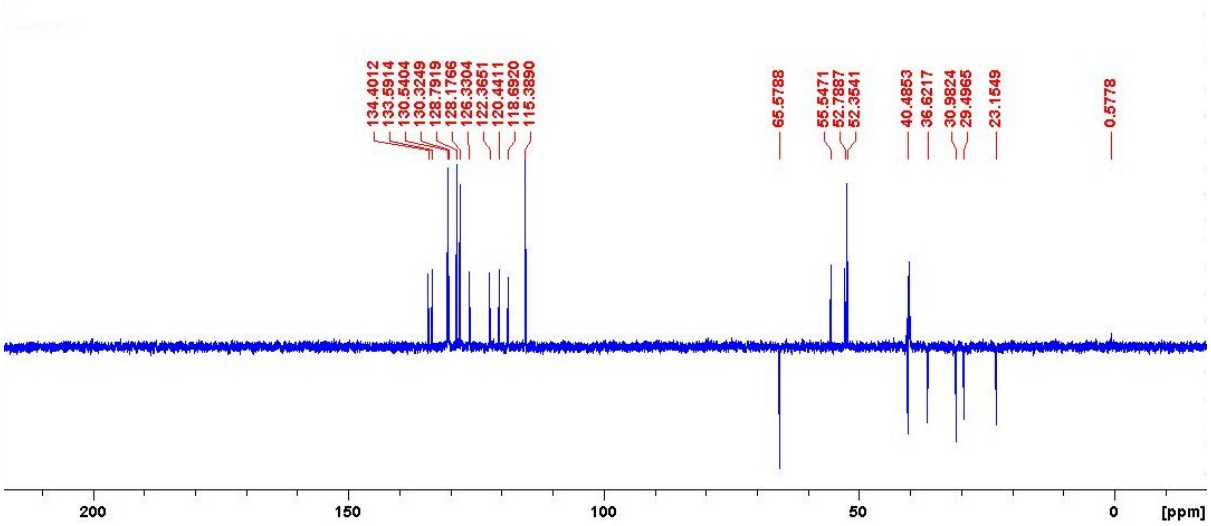

Figure S30. DEPT-135 NMR spectrum of compound **16**.

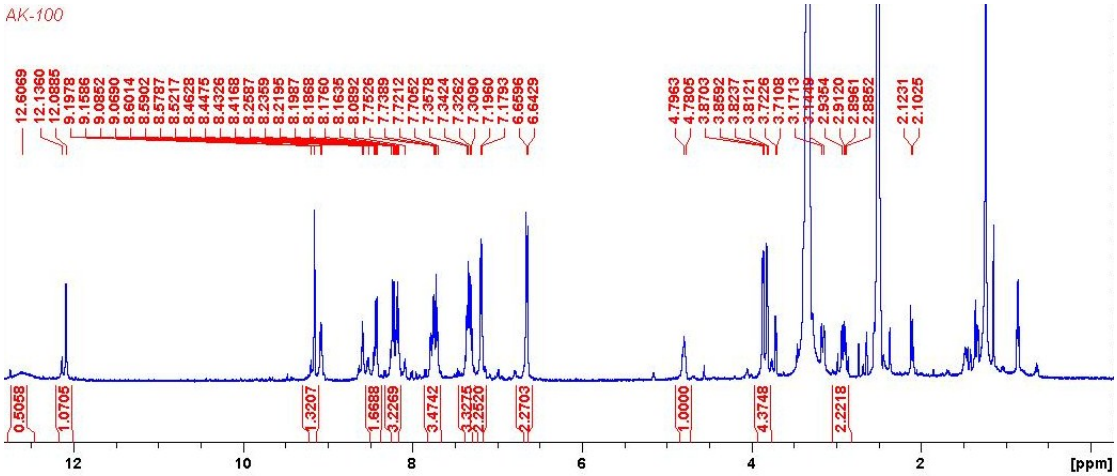

Figure S31. ^{1}H NMR spectrum of compound **18**.

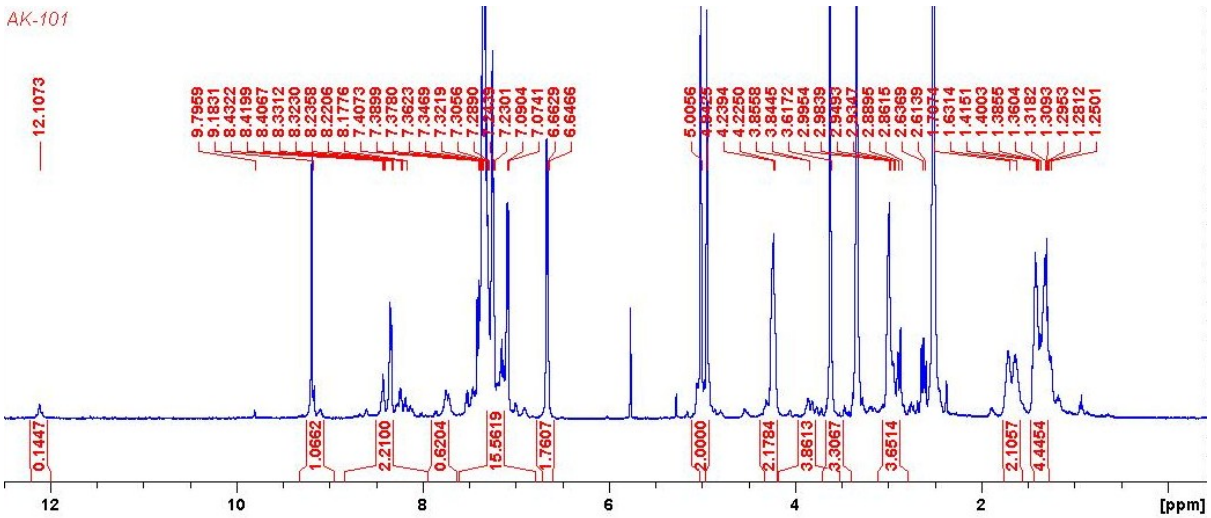

Figure S32. ^{1}H NMR spectrum of compound **19**.

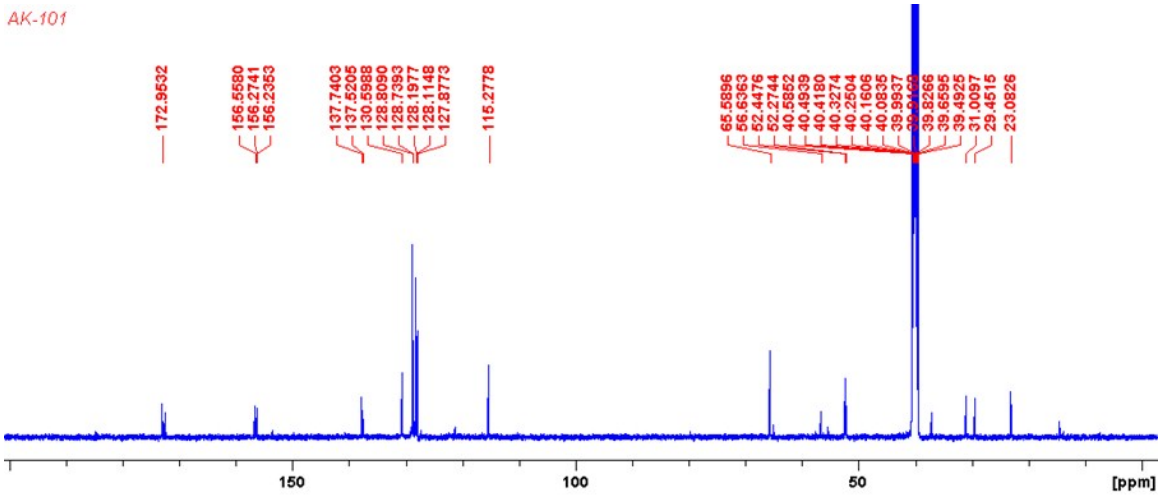

Figure S33. ^{13}C NMR spectrum of compound **19**.

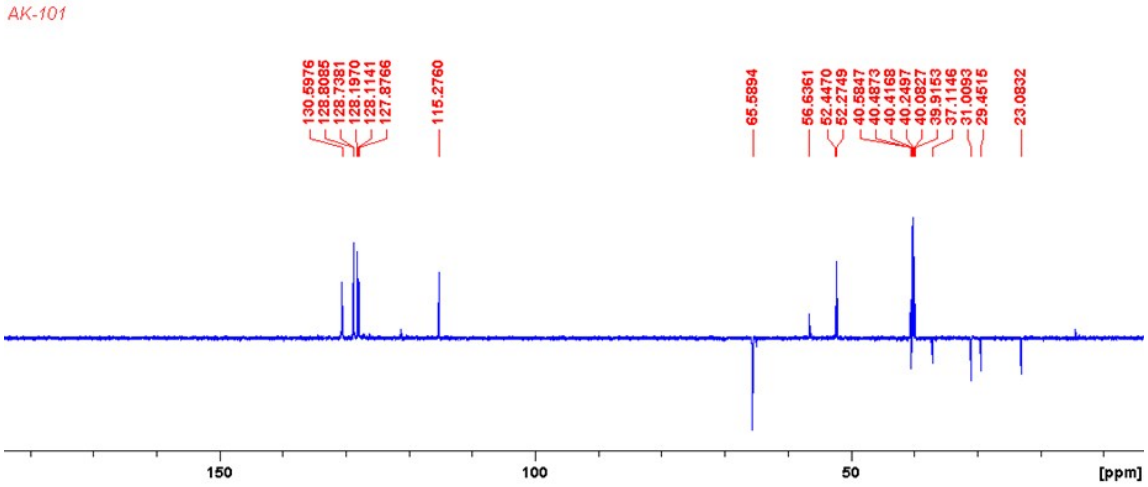

Figure S34. DEPT-135 NMR spectrum of compound **19**.

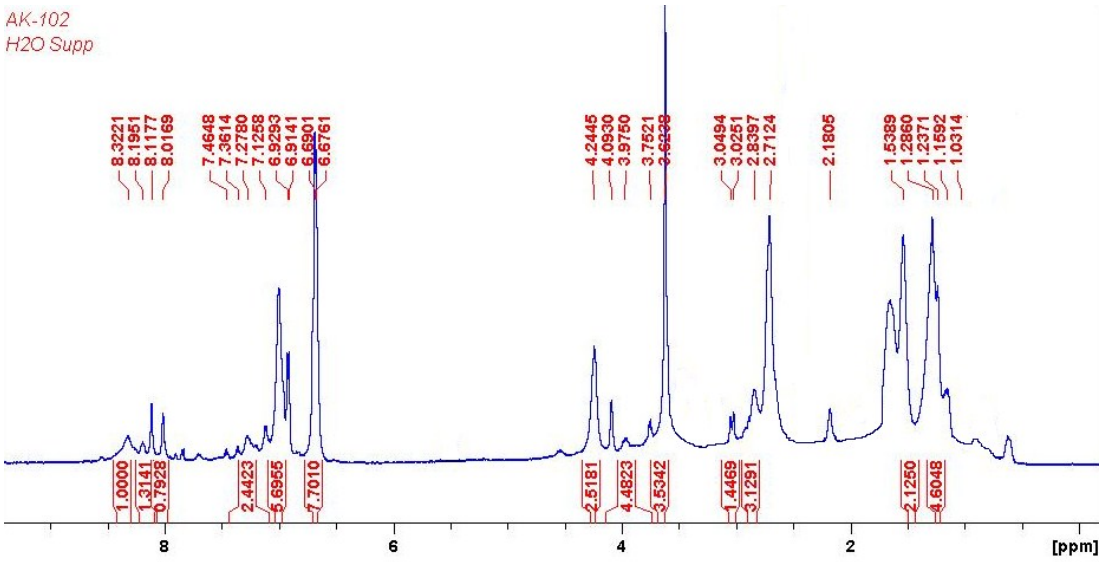

Figure S35. ^{1}H NMR spectrum of compound **6**.

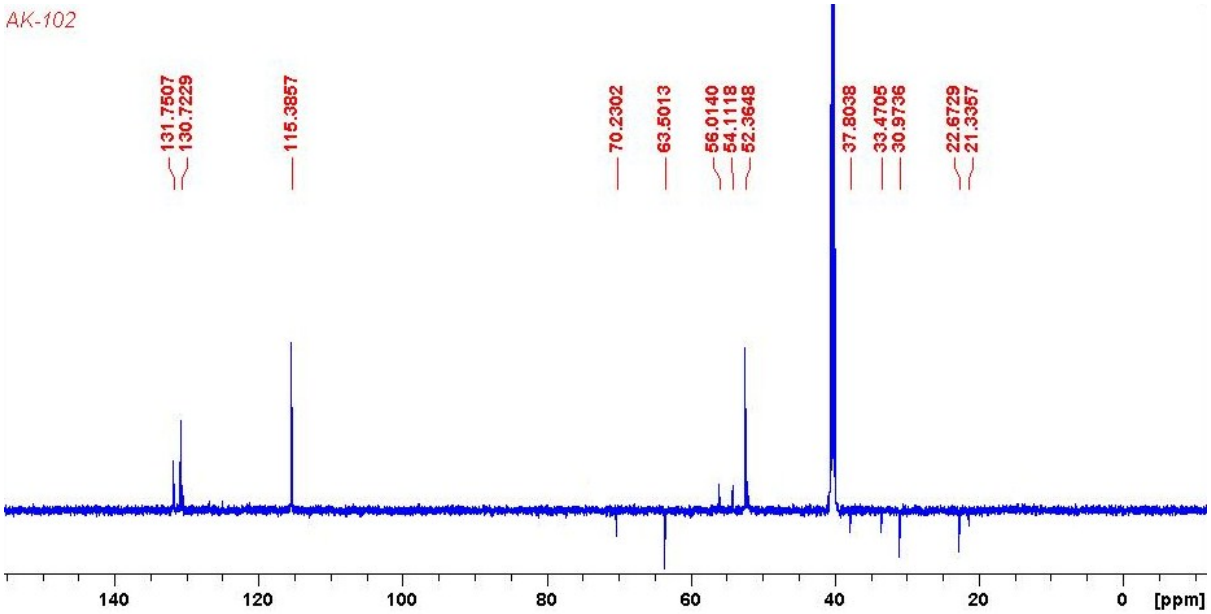

Figure S36. DEPT-135 NMR spectrum of compound **6**.

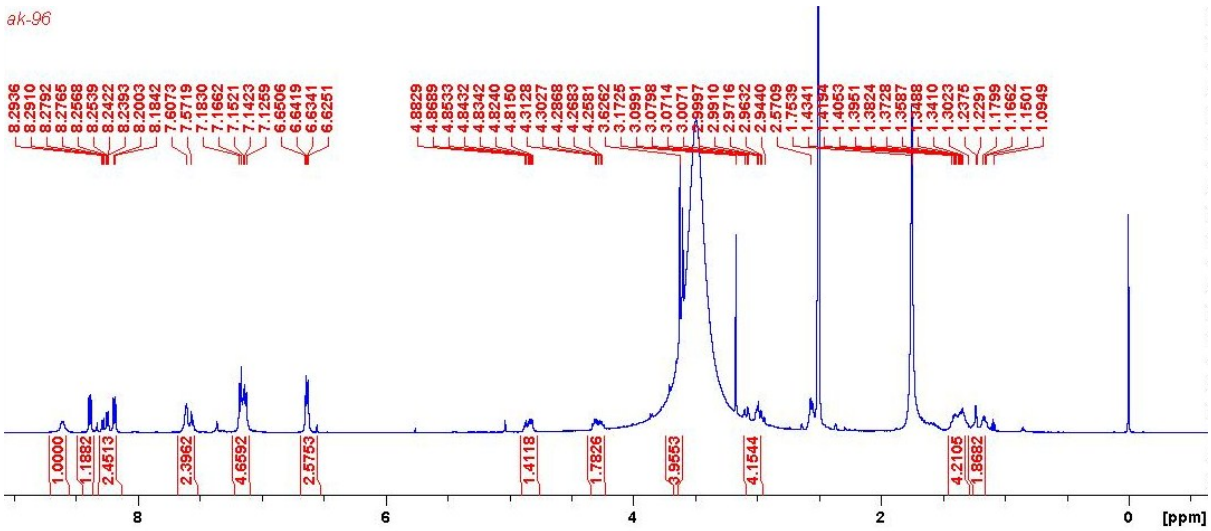

Figure S37. ^{1}H NMR spectrum of compound **4**.

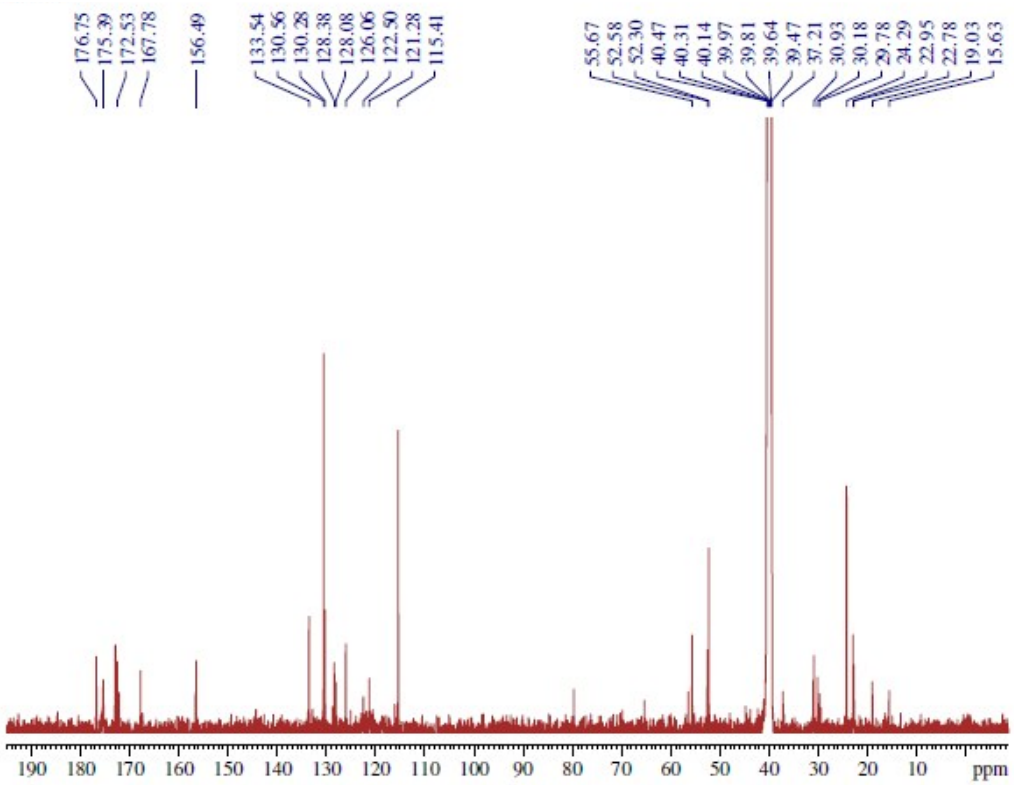

Figure S38. ^{13}C NMR spectrum of compound **4**.

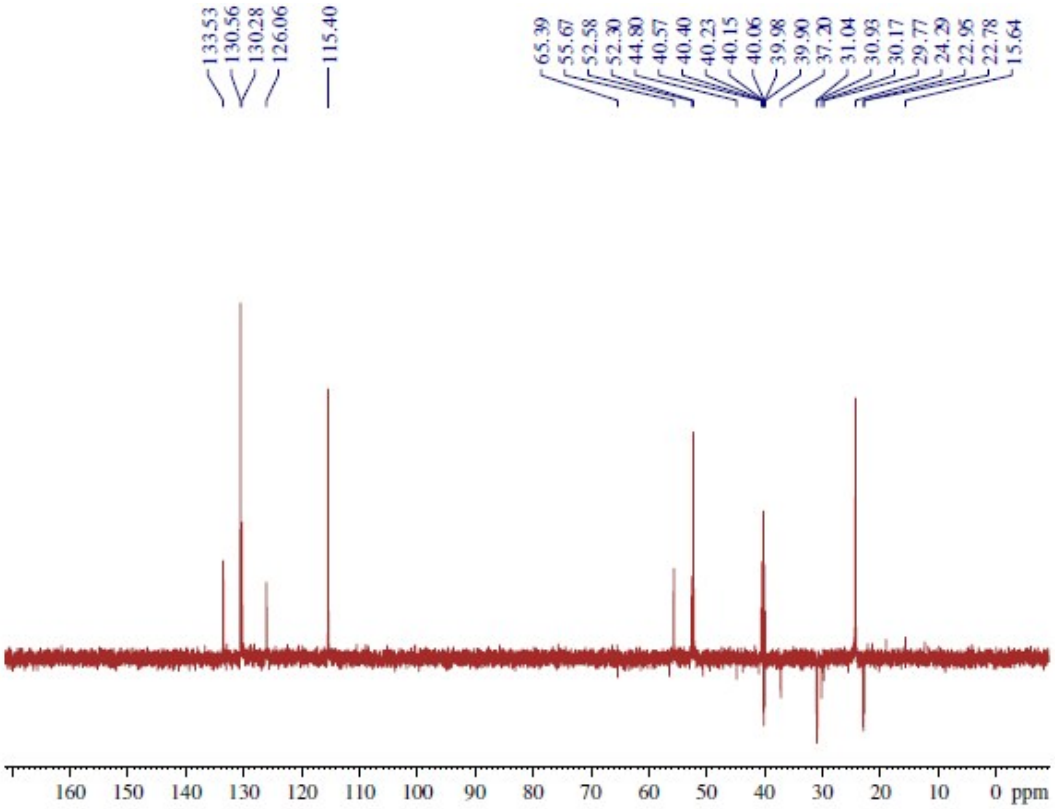

Figure S39. DEPT-135 NMR spectrum of compound **4**.

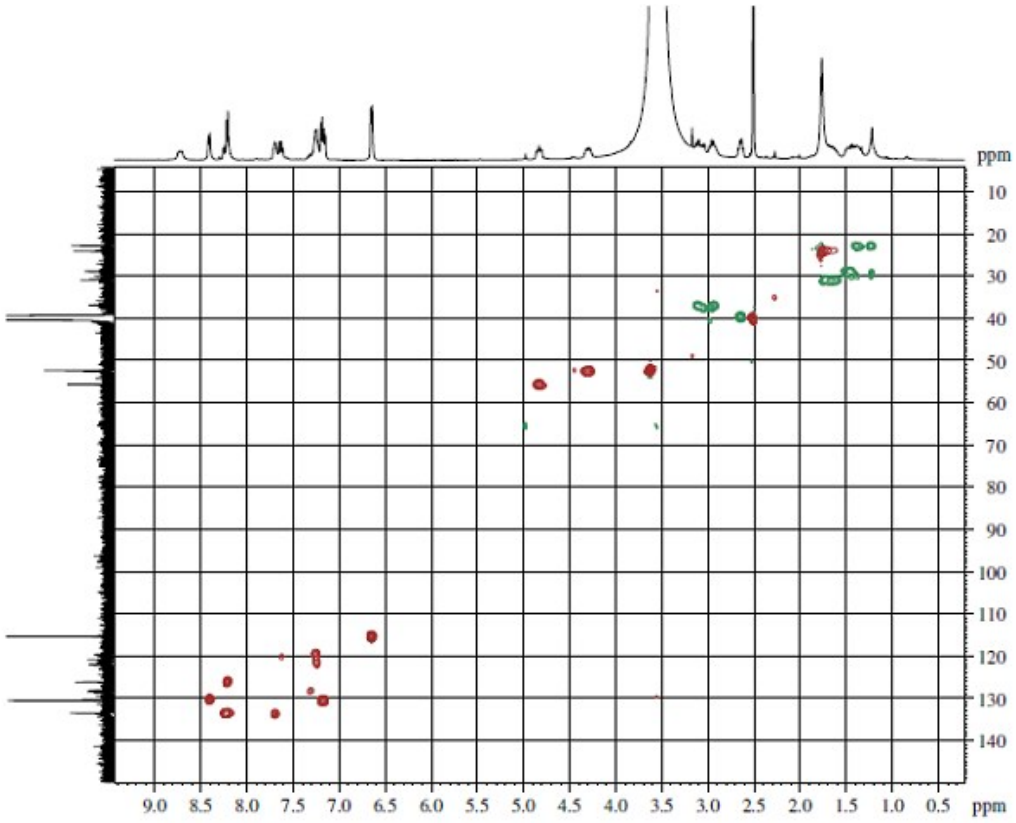

Figure S40. HSQC NMR spectrum of compound **4**.

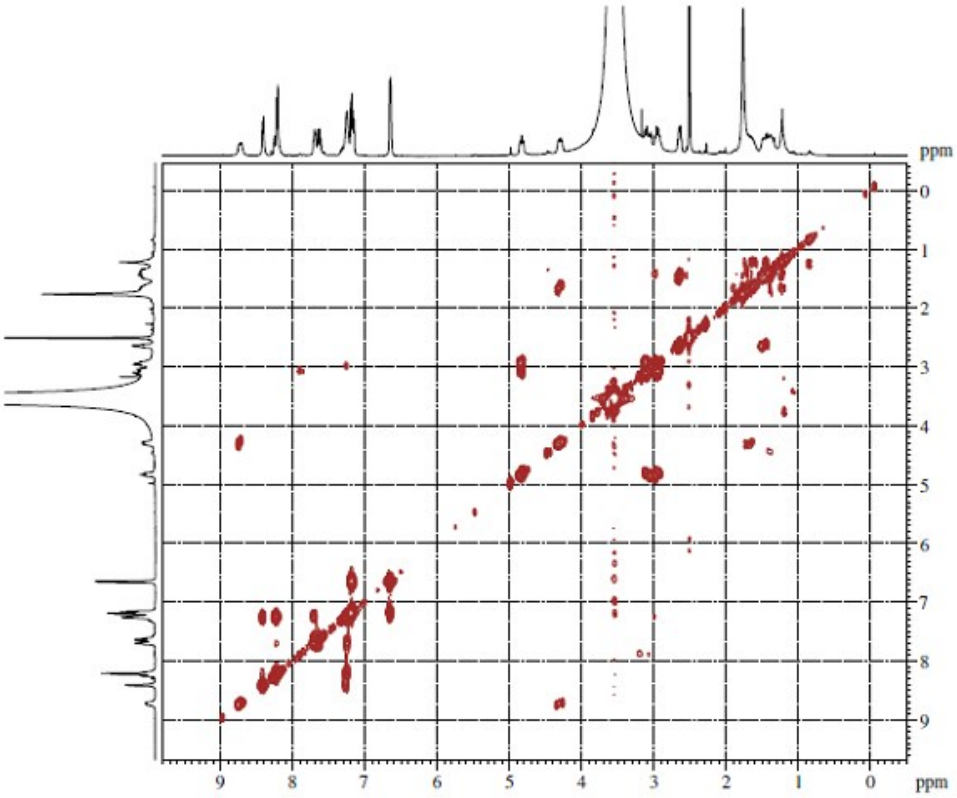

Figure S41. ^{1}H-^{1}H COSY NMR spectrum of compound **4**.

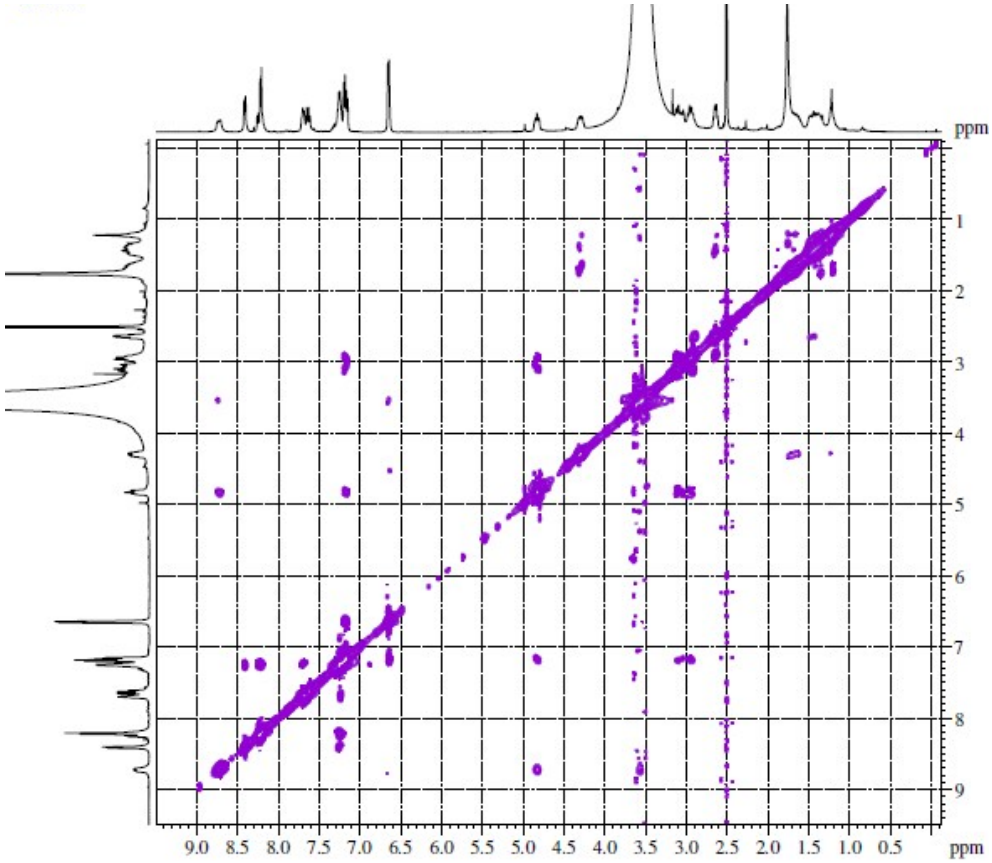

Figure S42. ^{1}H-^{1}H ROESY NMR spectrum of compound **4**.

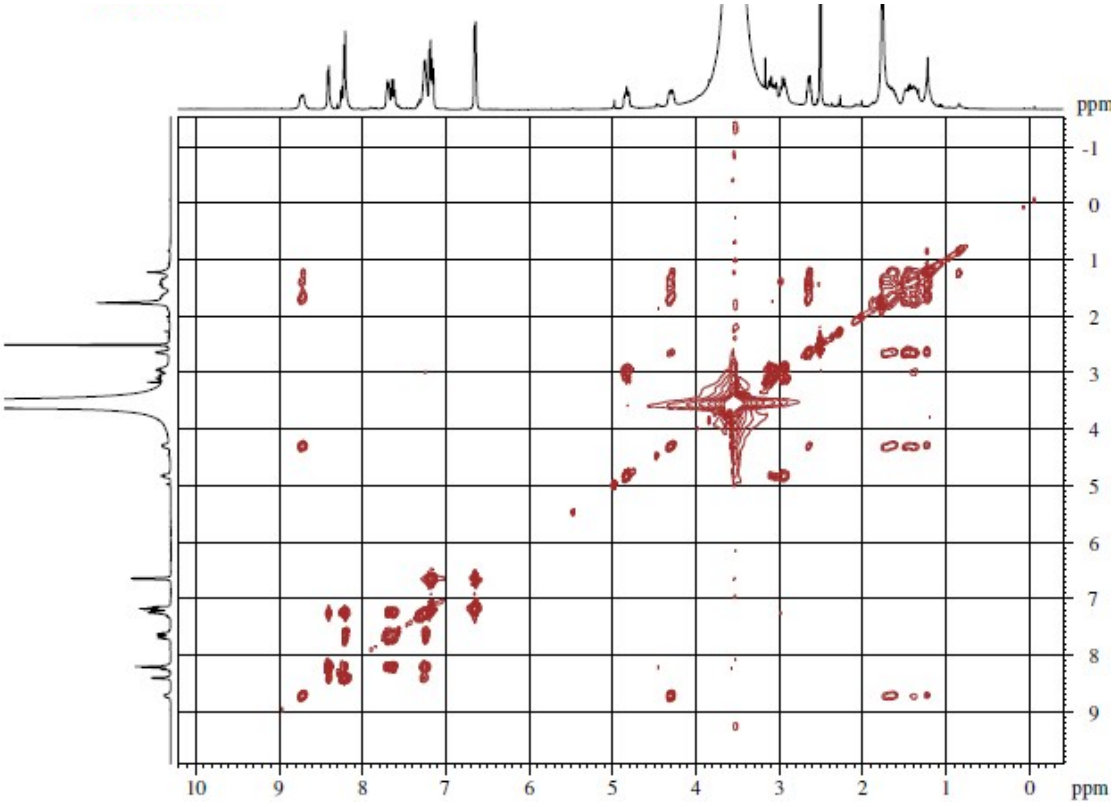

Figure S43. ^{1}H-^{1}H TOCSY NMR spectrum of compound **4**.

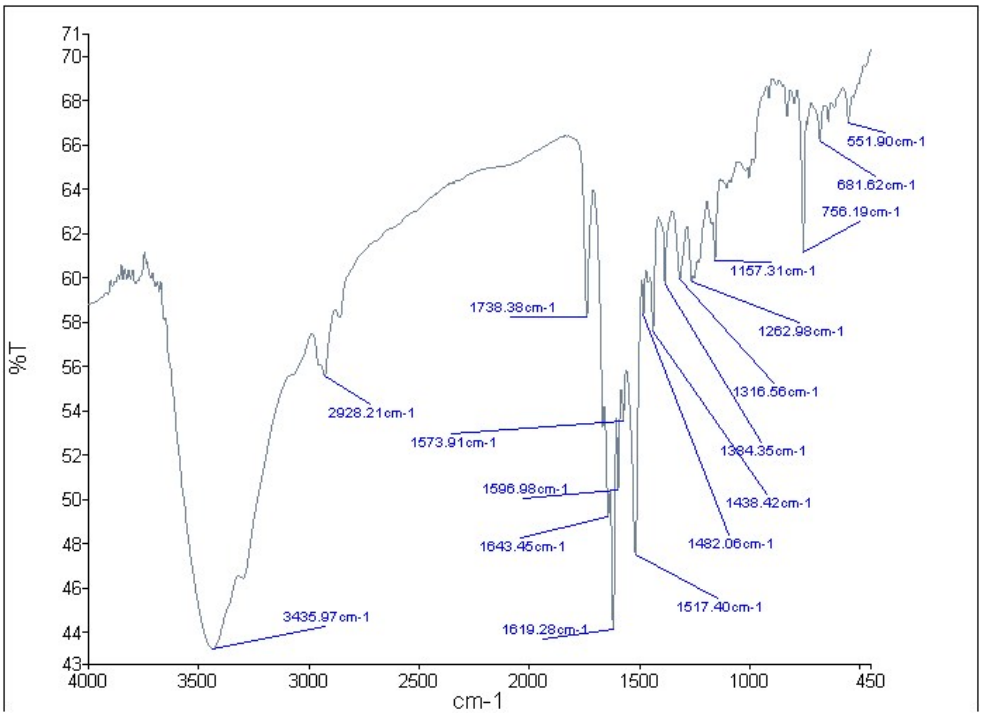

Figure S44. IR spectrum of compound **4**.

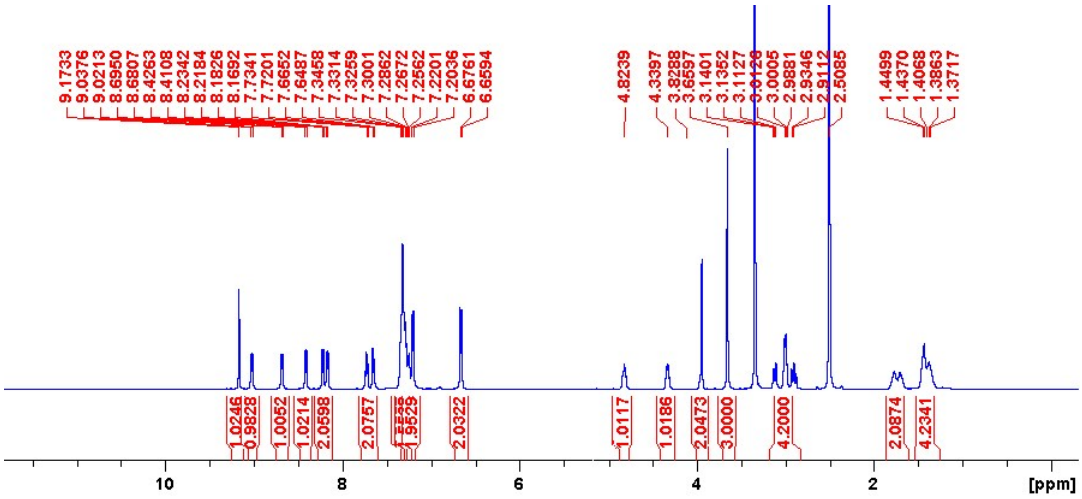

Figure S45. ^{1}H NMR spectrum of compound **5**.

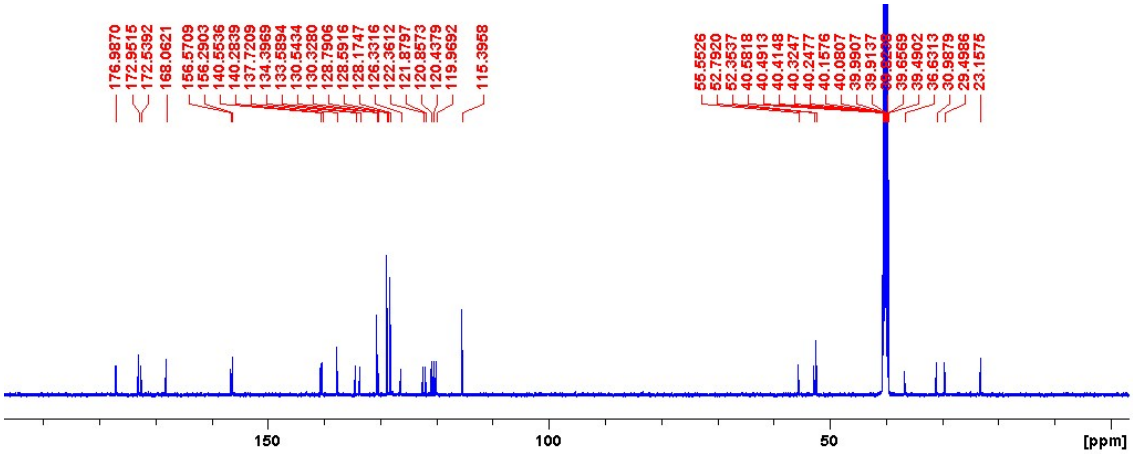

Figure S46. ^{13}C NMR spectrum of compound **5**.

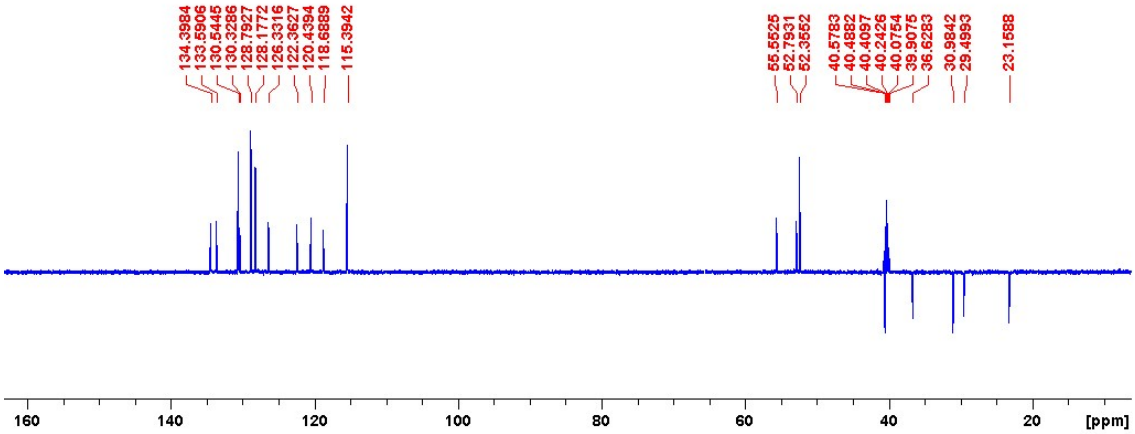

Figure S47. DEPT-135 NMR spectrum of compound **5**.

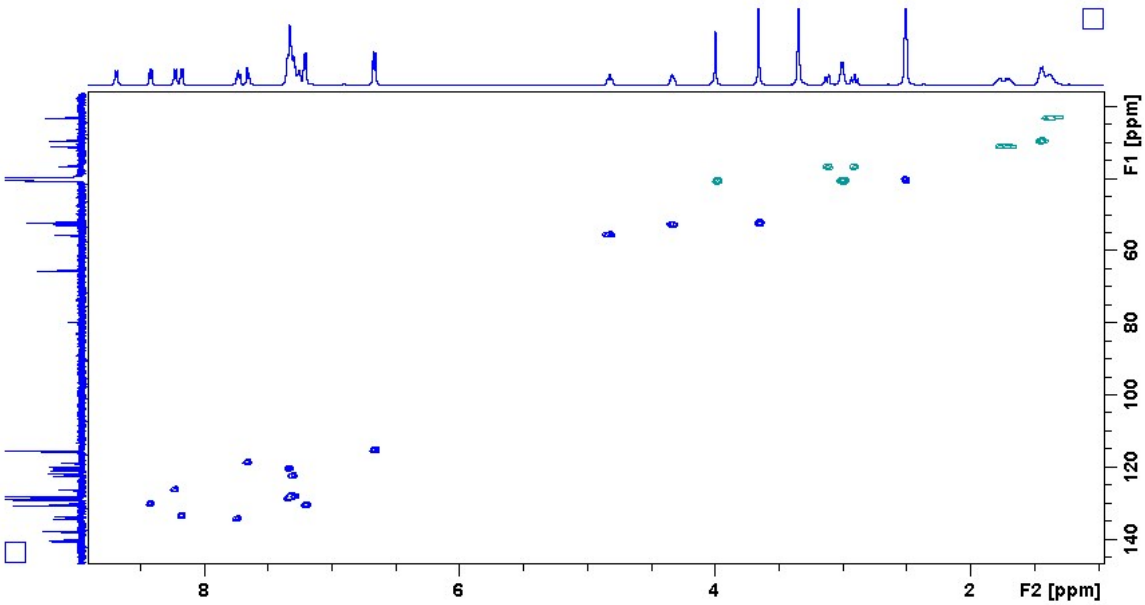

Figure S48. HSQC NMR spectrum of compound **5**.

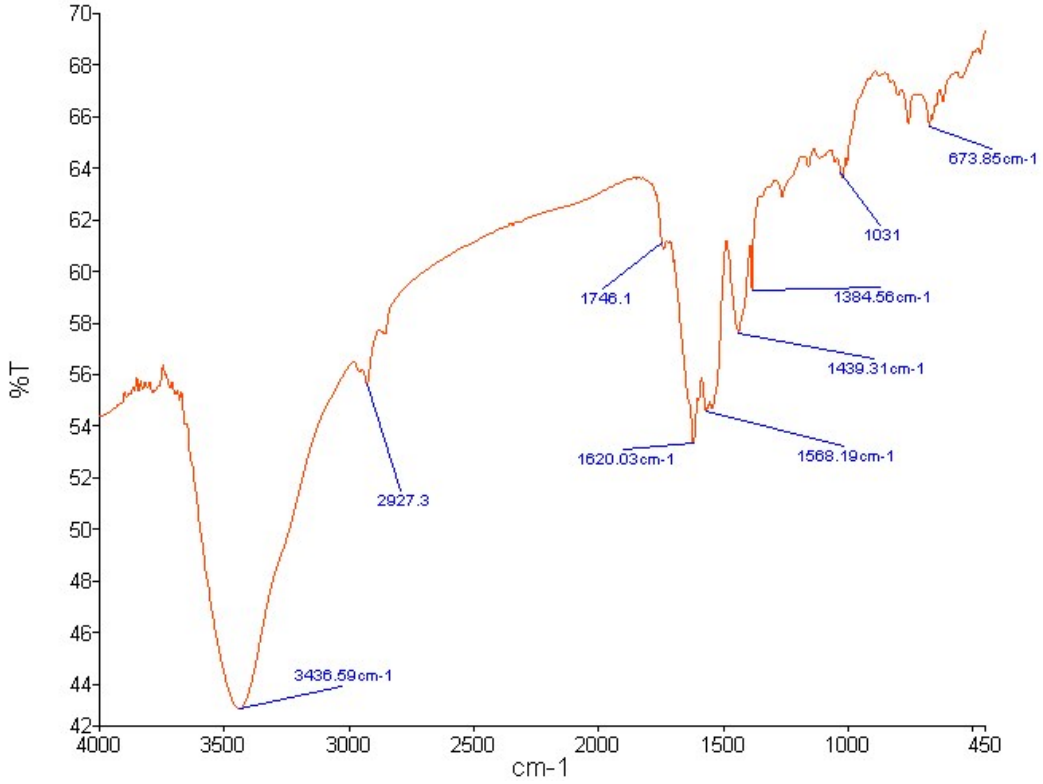

Figure S49. IR spectrum of compound **5**.

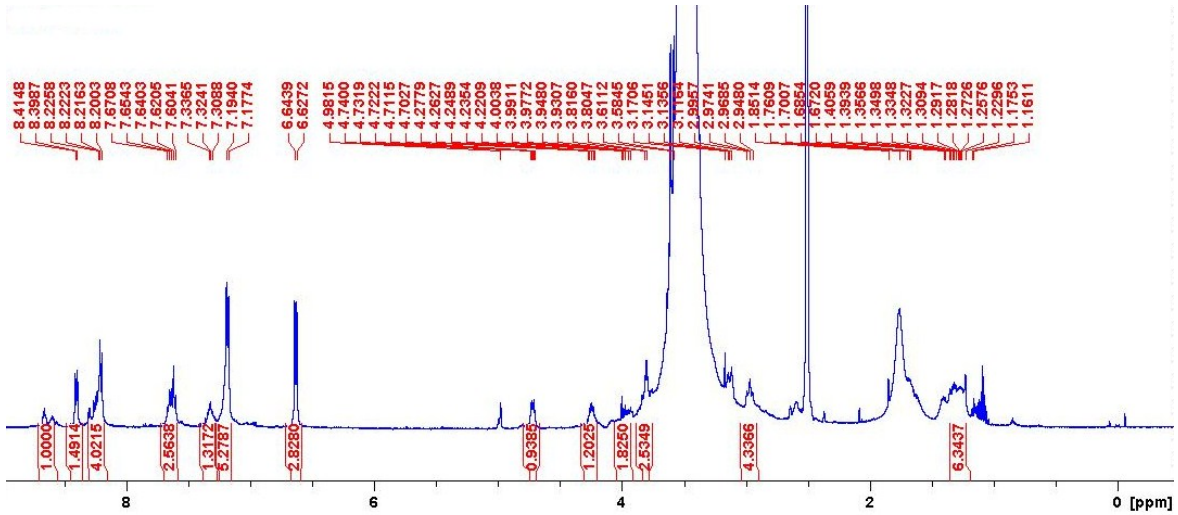

Figure S50. ^{1}H NMR spectrum of compound **7.**

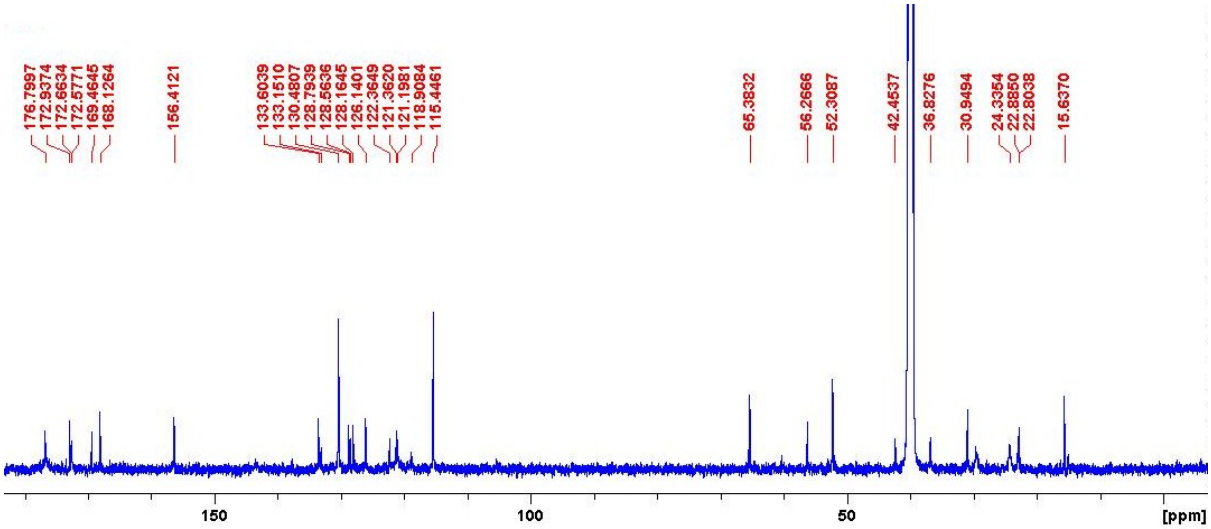

Figure S51. ^{13}C NMR spectrum of compound **7**.

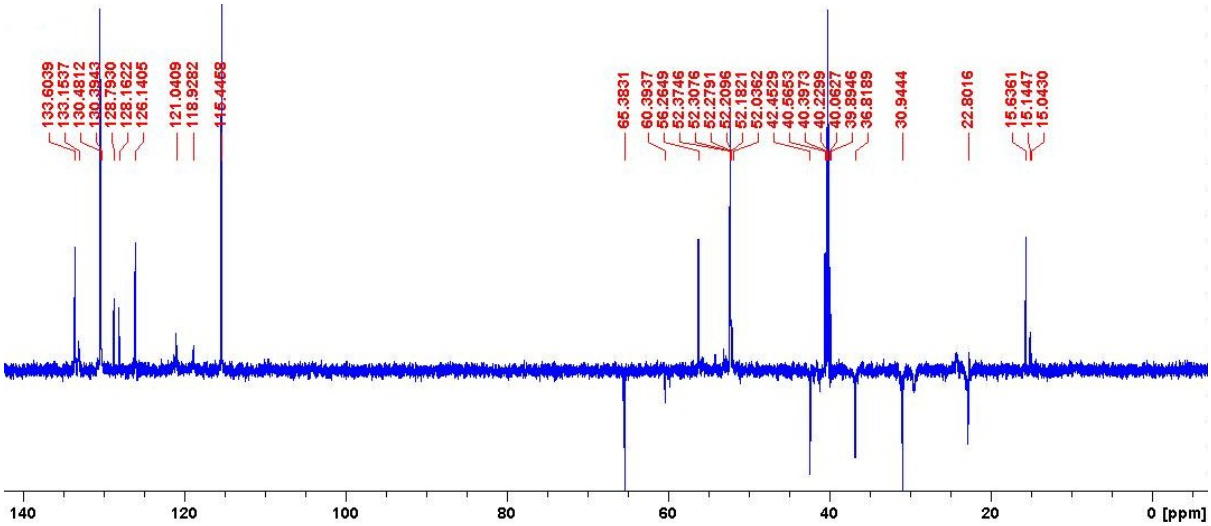

Figure S52. DEPT-135 NMR spectrum of compound **7**.

High Resoltion Mass Spectra

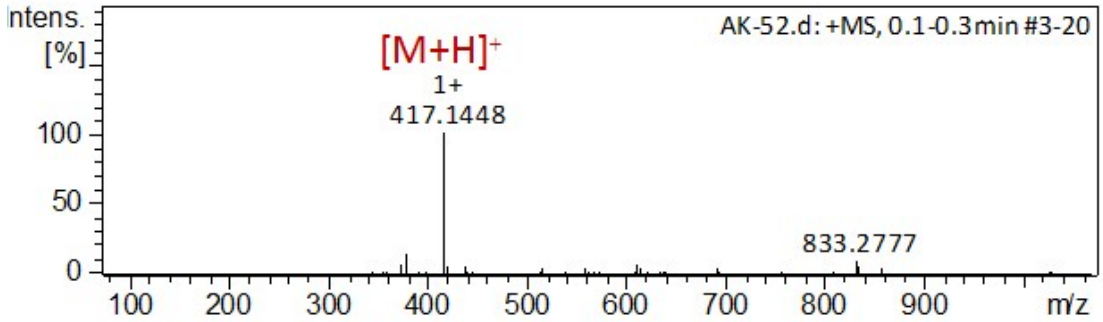

Figure S53. Mass spectrum of compound **11** (calcd *m/z* 417.1444, $[M+H]^+$).

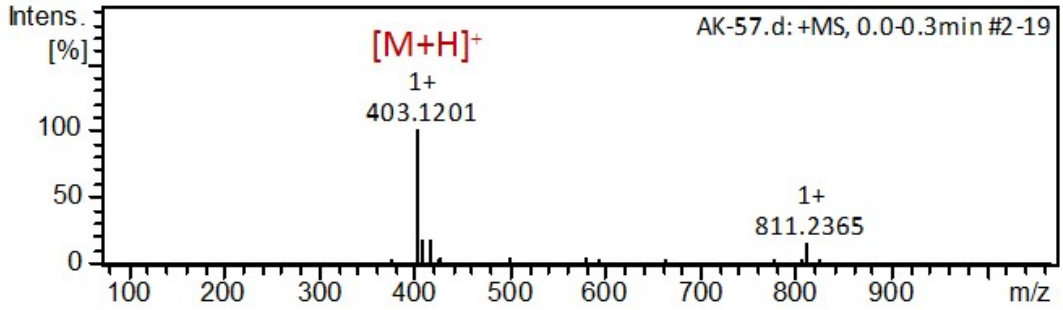

Figure S54. Mass spectrum of compound **12** (calcd *m/z* 403.1288, $[M+H]^+$).

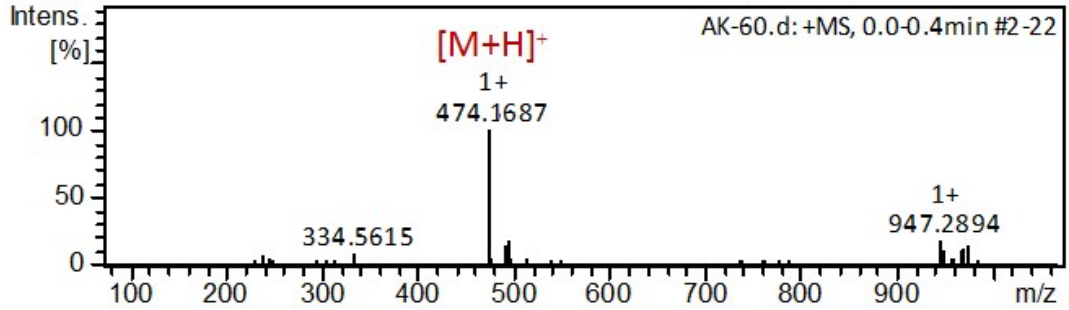

Figure S55. Mass spectrum of compound **13** (calcd *m/z* 474.1659, $[M+H]^+$).

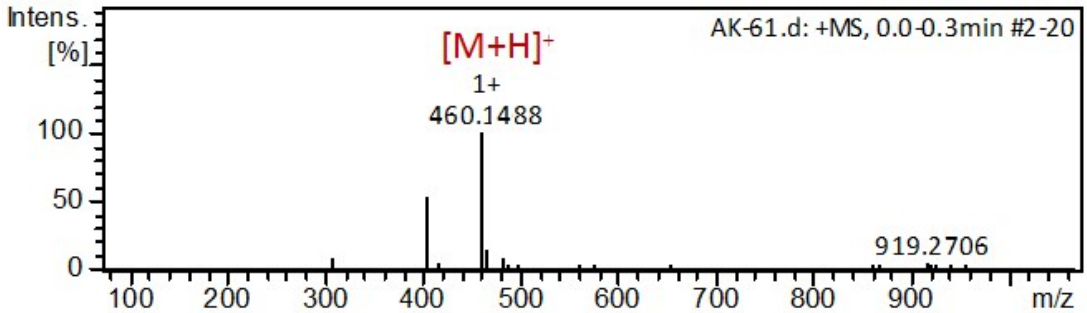

Figure S56. Mass spectrum of compound **14** (calcd *m/z* 460.1503, $[M+H]^+$).

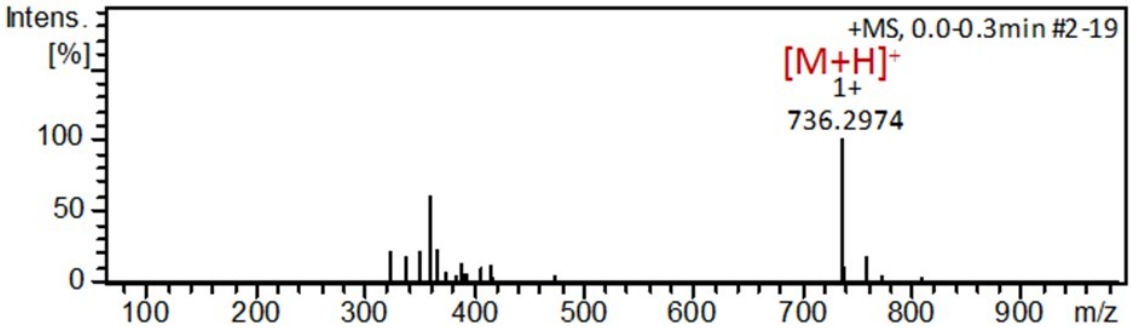

Figure S57. Mass spectrum of compound **15** (calcd *m/z* 736.2977, $[M+H]^+$).

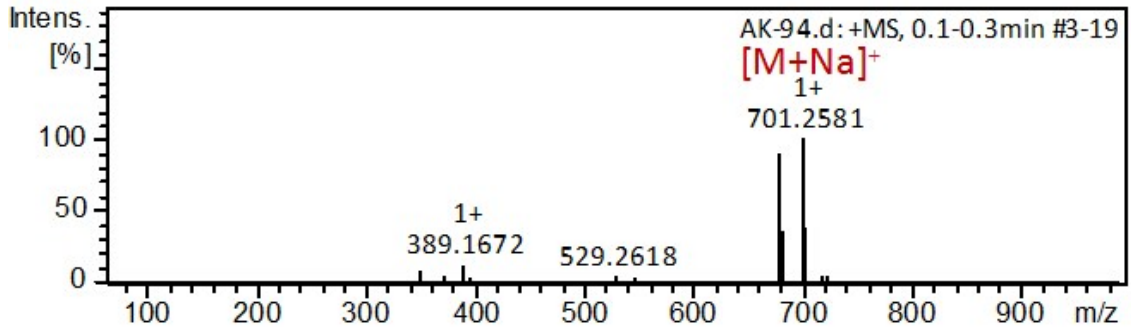

Figure S58. Mass spectrum of compound **16** (calcd *m/z* 701.2581, $[M+H]^+$).

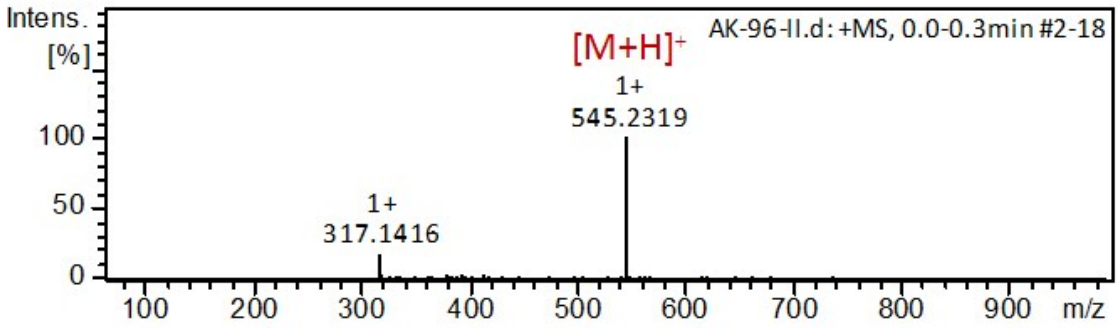

Figure S59. Mass spectrum of compound **4** (calcd *m/z* 545.2394, $[M+H]^+$).

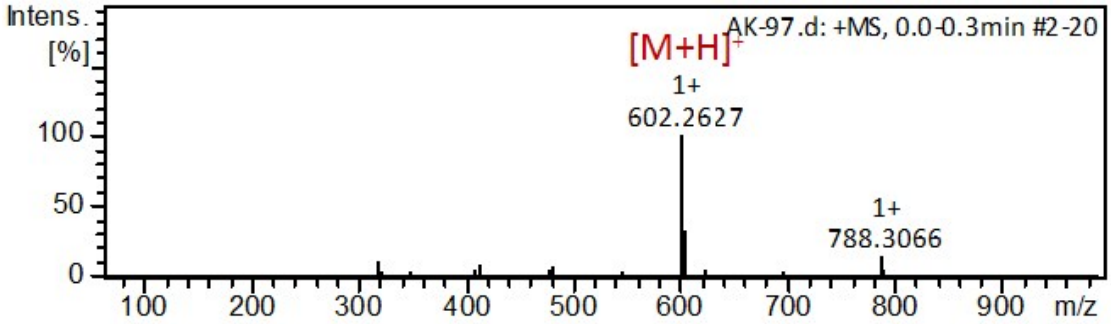

Figure S60. Mass spectrum of compound **5** (calcd *m/z* 502.2609, $[M+H]^+$).

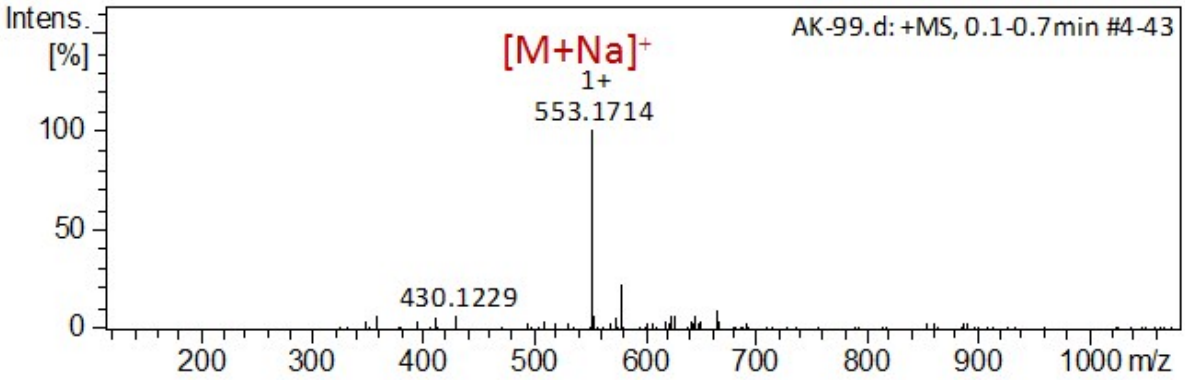

Figure S61. Mass spectrum of compound **17** (calcd *m/z* 553.1714, $[M+Na]^+$).

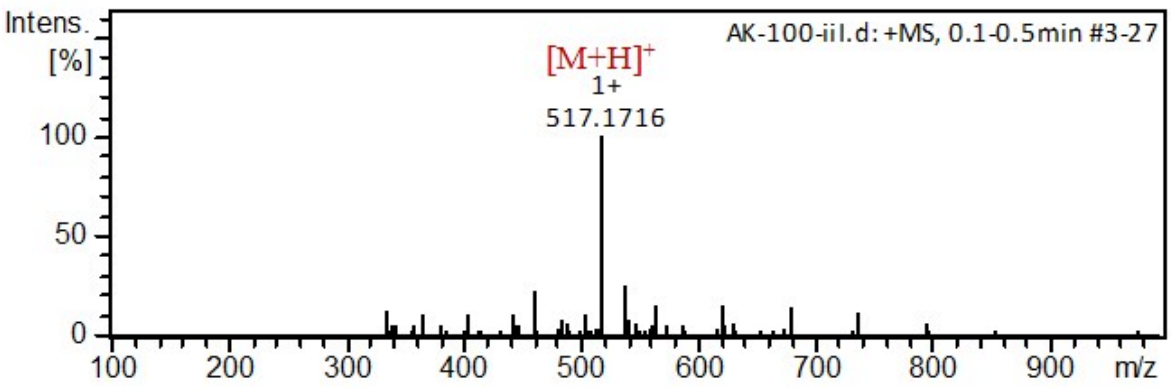

Figure S62. Mass spectrum of compound **18** (calcd *m/z* 517.1717, $[M+H]^+$).

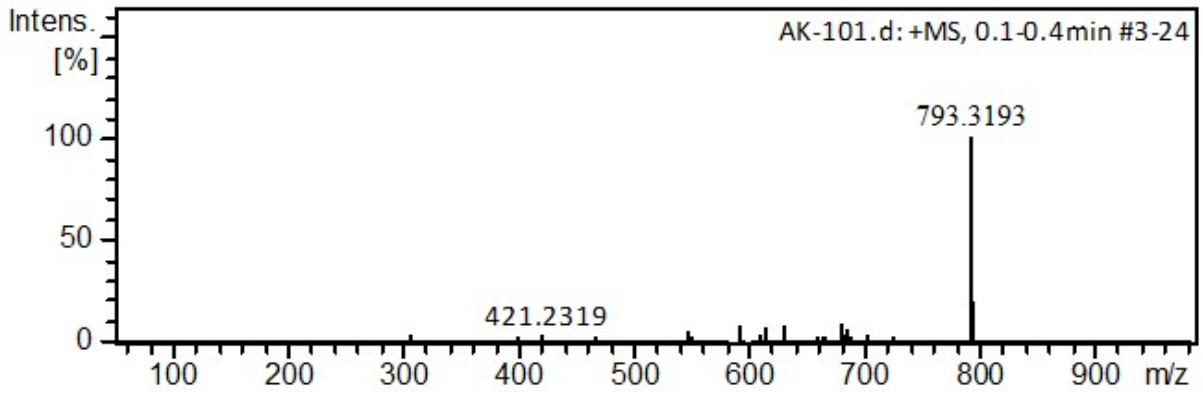

Figure S63. Mass spectrum of compound **19** (calcd *m/z* 793.3191 $[M+H]^+$).

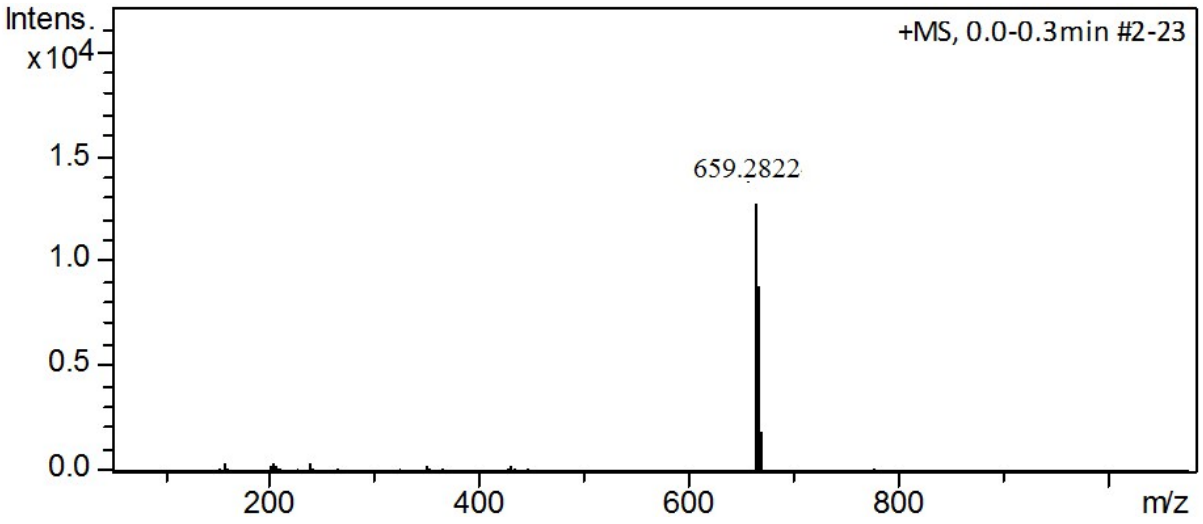

Figure S64. Mass spectrum of compound **6** (calcd *m/z* 659.2823 $[M+H]^+$).

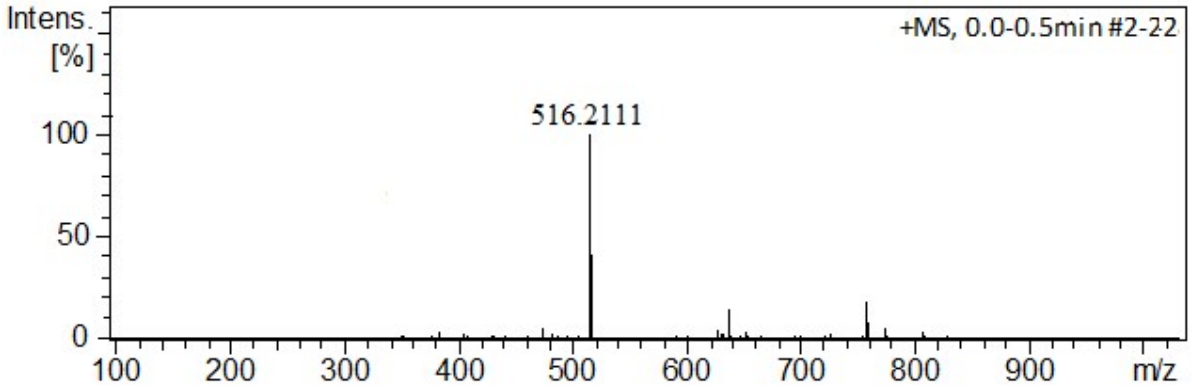

Figure S65. Mass spectrum of compound **20** (calcd *m/z*, 516.2129 $[M+H]^+$).

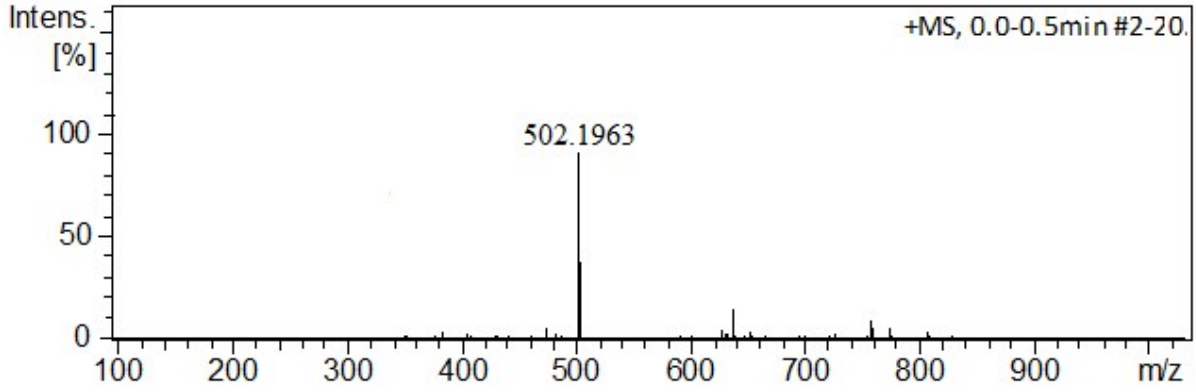

Figure S66. Mass spectrum of compound **21** (calcd *m/z*, 502.1972 $[M+H]^+$).

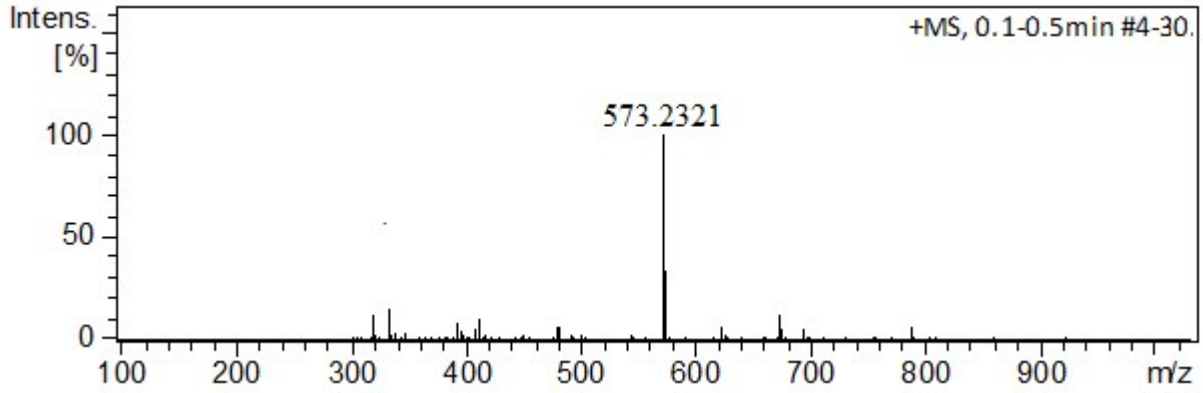

Figure S67. Mass spectrum of compound **22** (calcd *m/z*, 573.2343 $[M+H]^+$).

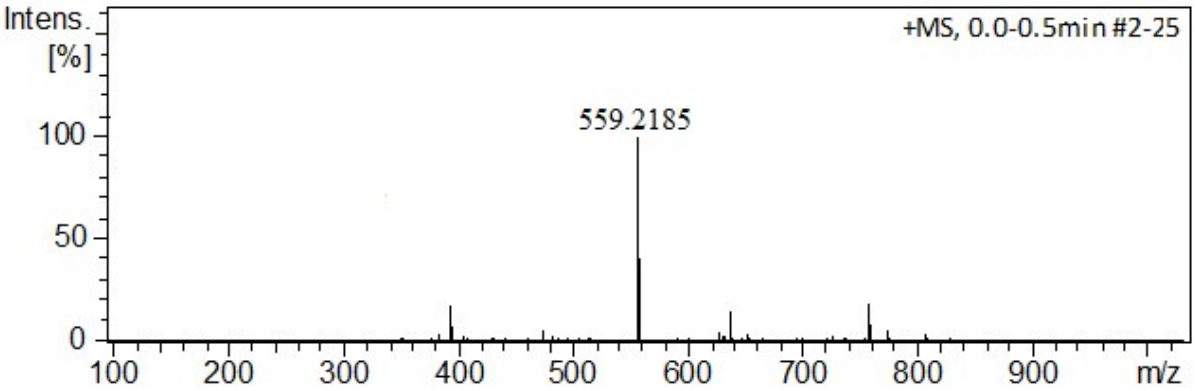

Figure S68. Mass spectrum of compound **23** (calcd *m/z*, 559.2187 $[M+H]^+$).

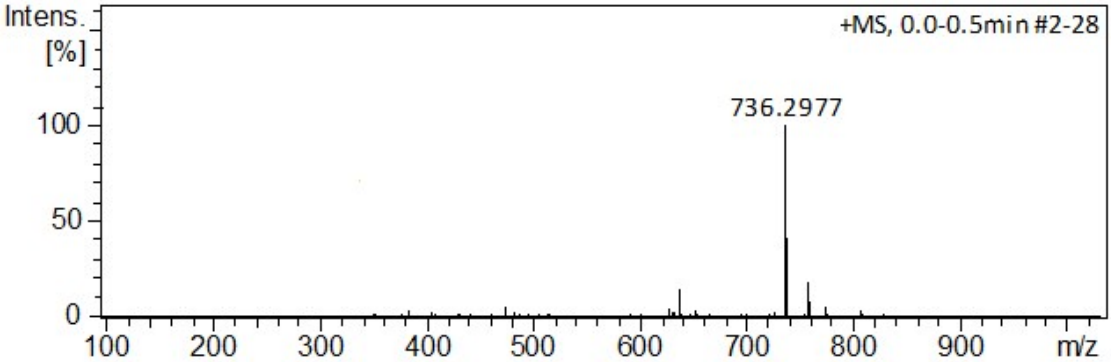

Figure S69. Mass spectrum of compound **24** (calcd *m/z* 736.2977, $[M+H]^+$).

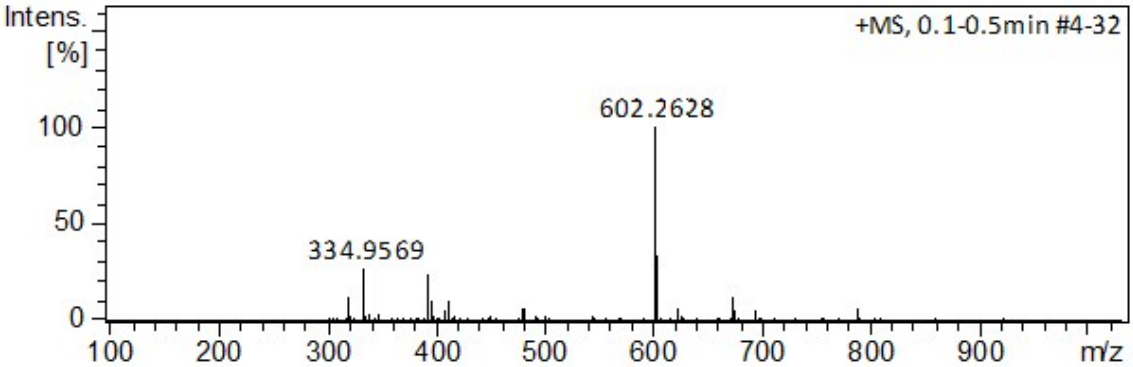

Figure S70. Mass spectrum of compound **7** (calcd *m/z* 602.2609, $[M+H]^+$).

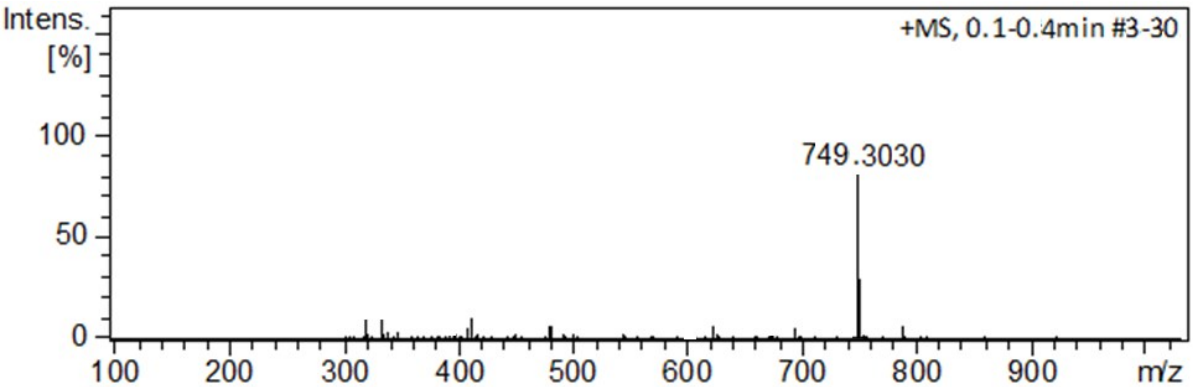

Figure S71. Mass spectrum of compound **25** (calcd *m/z* 749.3035, $[M+H]^+$).

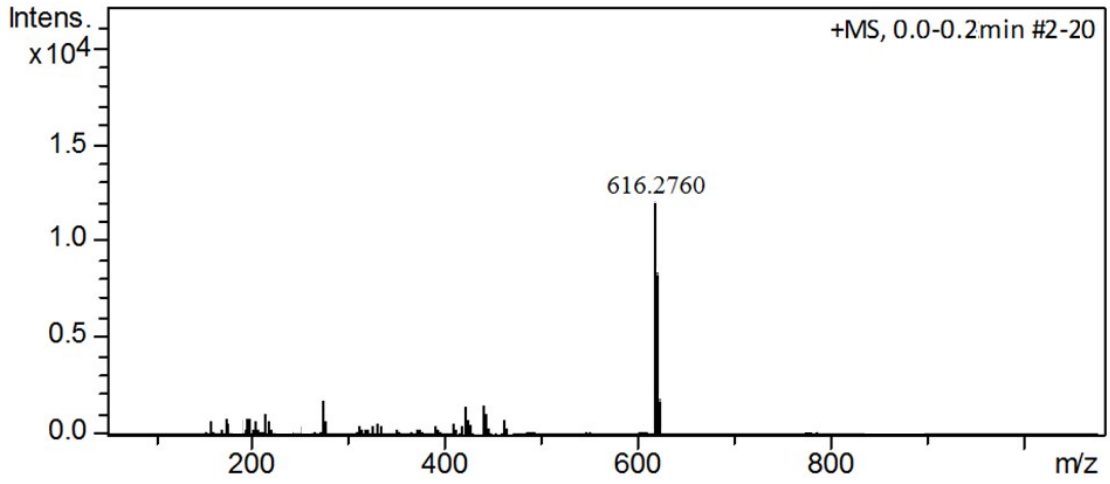

Figure S72. Mass spectrum of compound **26** (calcd *m/z* 616.2766, $[M+H]^+$).

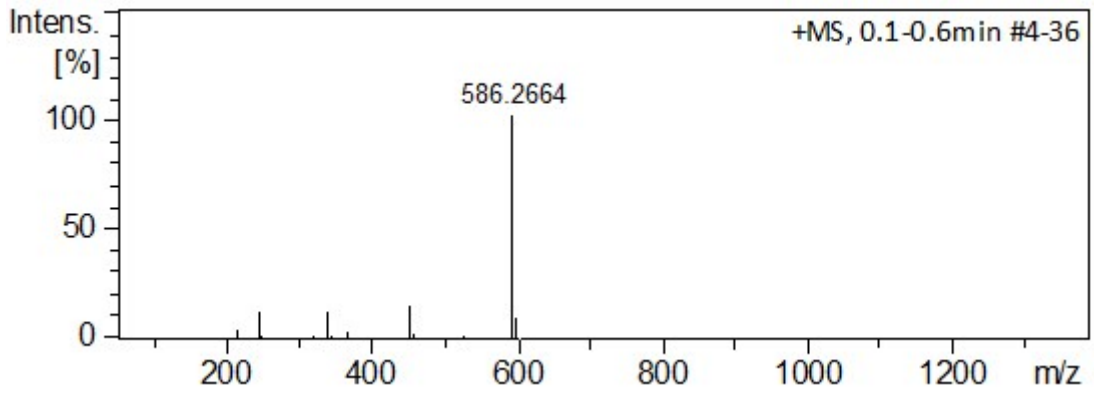

Figure S73. Mass spectrum of compound **27** (calcd *m/z* 586.2660, $[M+H]^+$).

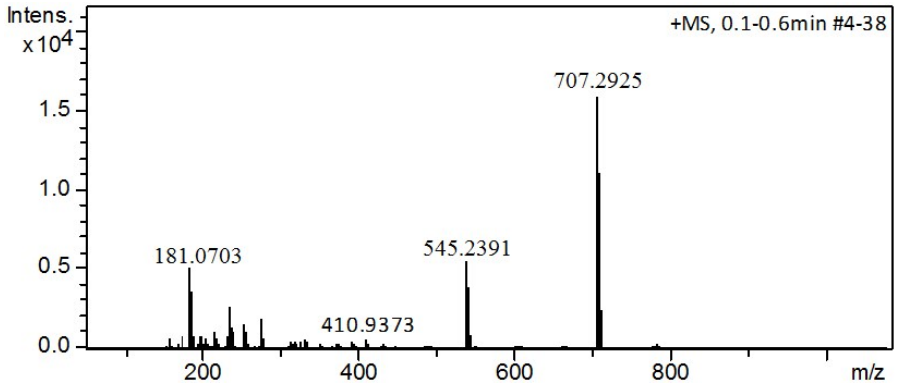

Figure S74. Mass spectrum of reaction mixture of compound **4** and D-fructose. Peak at *m/z* 707.2925 corresponds to mass of Schiff base ions (calcd *m/z* 707.2923, $[M]^+$). Peaks at *m/z* 181.0703 and 545.2391 correspond to *m/z* of fructose and compound **4** ions, respectively.

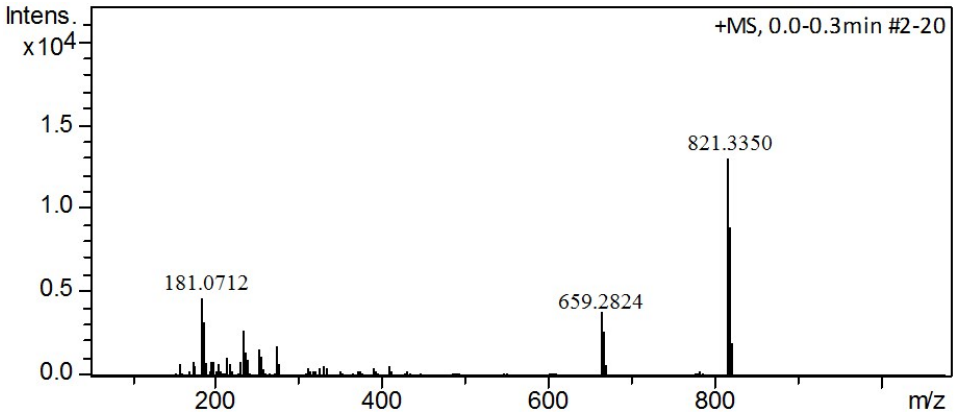

Figure S75. Mass spectrum of reaction mixture of compound **6** and D-fructose. Peak at *m/z* 821.3350 corresponds to mass of Schiff base ions (calcd *m/z* 821.3352, $[M]^+$). Peaks at *m/z* 181.0712 and 659.2824 correspond to *m/z* of fructose and compound **6** ions, respectively.

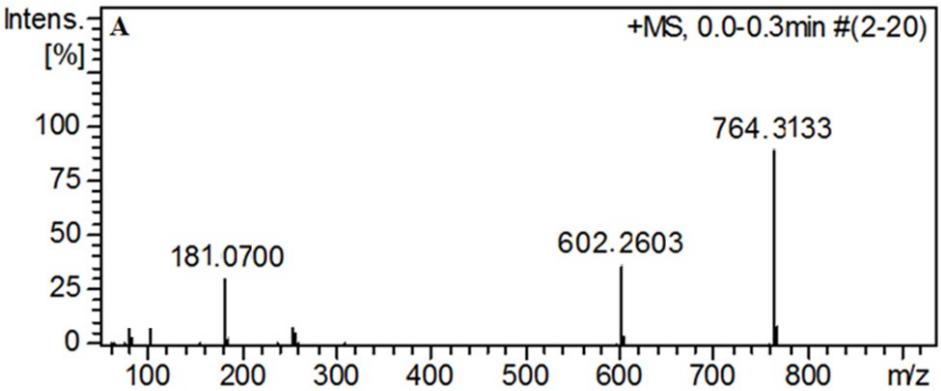

Figure S76. HRMS of the reaction mixture of compound **5d** and L-fructose after 60 min of stirring at 25 – 27 °C.

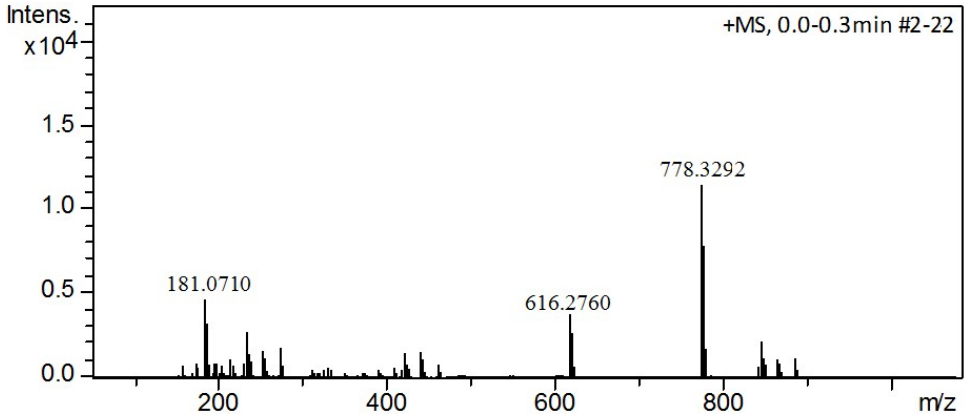

Figure S77. Mass spectrum of the reaction mixture of compound **26** (Scheme S5) and D-fructose. Peak at *m/z* 778.3292 corresponds to mass of Schiff base ions (calcd *m/z* 778.3294, $[M]^+$). Peaks at *m/z* 181.0710 and 616.2760 correspond to *m/z* of fructose and compound **26** ions (calcd *m/z* 616.2766, $[M+H]^+$), respectively.

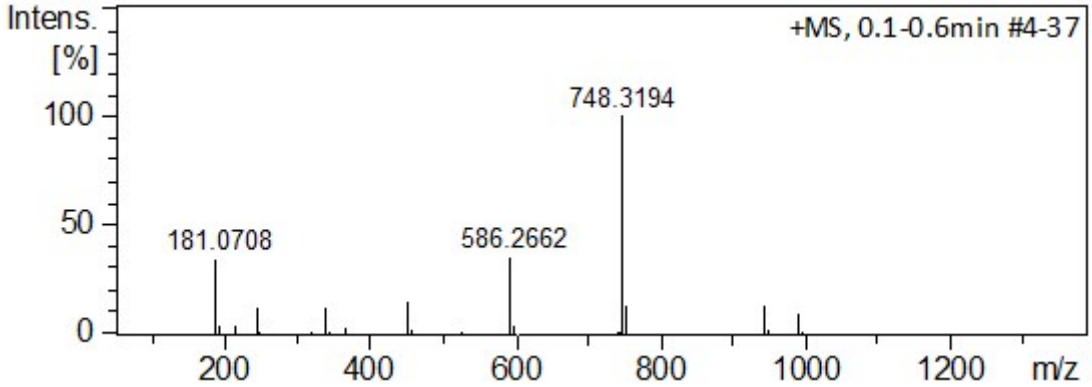

Figure S78. Mass spectrum of the reaction mixture of compound **27** (Scheme S6) and D-fructose. Peak at *m/z* 748.3194 corresponds to mass of Schiff base ions (calcd *m/z* 748.3188, $[M]^+$). Peaks at *m/z* 181.0708 and 586.2662 correspond to *m/z* of fructose and compound **27** ions (calcd *m/z* 586.2660, $[M+H]^+$), respectively.

Procedure for Energy minimization of compounds[2]

Compounds were built in the workspace of ArgusLab 4.0.1 and energy minimized using PM3 basis set. For each compound, 20,000 iterations and maximum 20,000 steps were recorded to get the optimized geometry of the molecule.

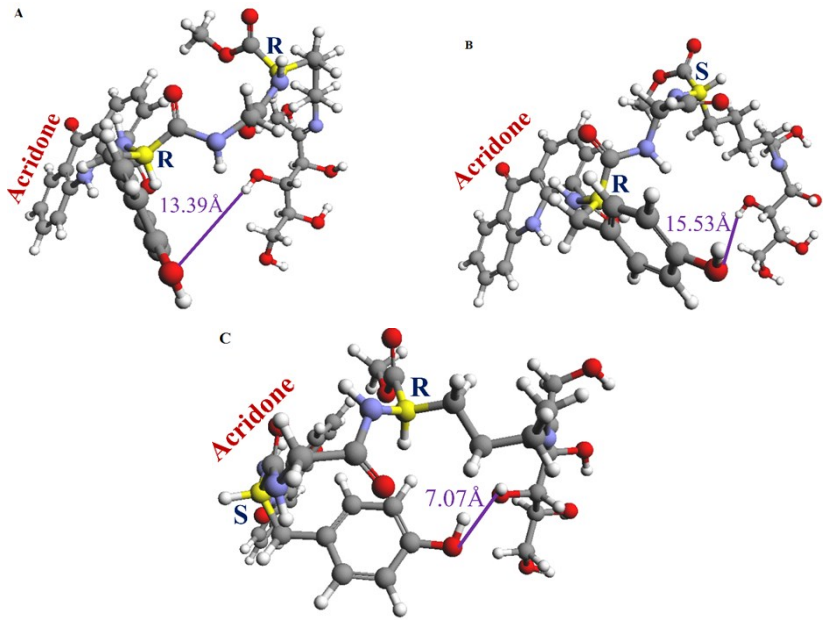

Figure S79. Energy minimized structures of Schiff bases obtained from (A) compound **5a**, (B) compound **5b** and (C) compound **5c**.

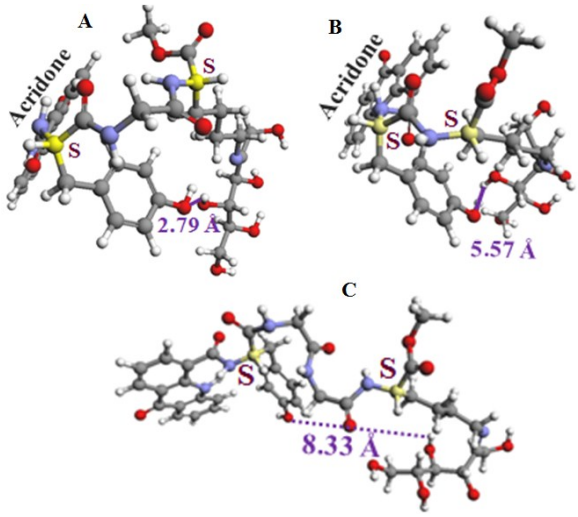

Figure S80. Energy minimized geometry of Schiff bases: A) Schiff base **8** showing 2.79 Å distance between phenolic O and C4-OH of fructose moiety, B) Schiff base corresponding to compound **4d**. Distance between phenolic O and C4-OH is 5.57 Å, C) Schiff base corresponding to compound **6d**. Distance between phenolic O and C4-OH is 8.33Å. In all the three Schiff bases, the asymmetric carbons are marked as yellow and each has S-configuration.

Energy minimized geometries of Schiff bases obtained from compounds **5d**, **4d** and **6d**, respectively supported the preferred cleavage of fructose by compound **5d**. The phenolic O in Schiff base **8** showed the proximity to C4-OH by 2.79 Å while in the case of Schiff bases of

compound **4d** and **5d**, this distance was 5.57 and 8.33 Å, respectively. In contrast to Schiff base **8**, its analogues obtained from compounds **5a**, **5b** and **5c**, carrying respectively *R, R*; *R, S* and *S, R* configurations at C_α of tyr and lys have phenolic O far away from C4-O**H** of fructose (Figure S78).

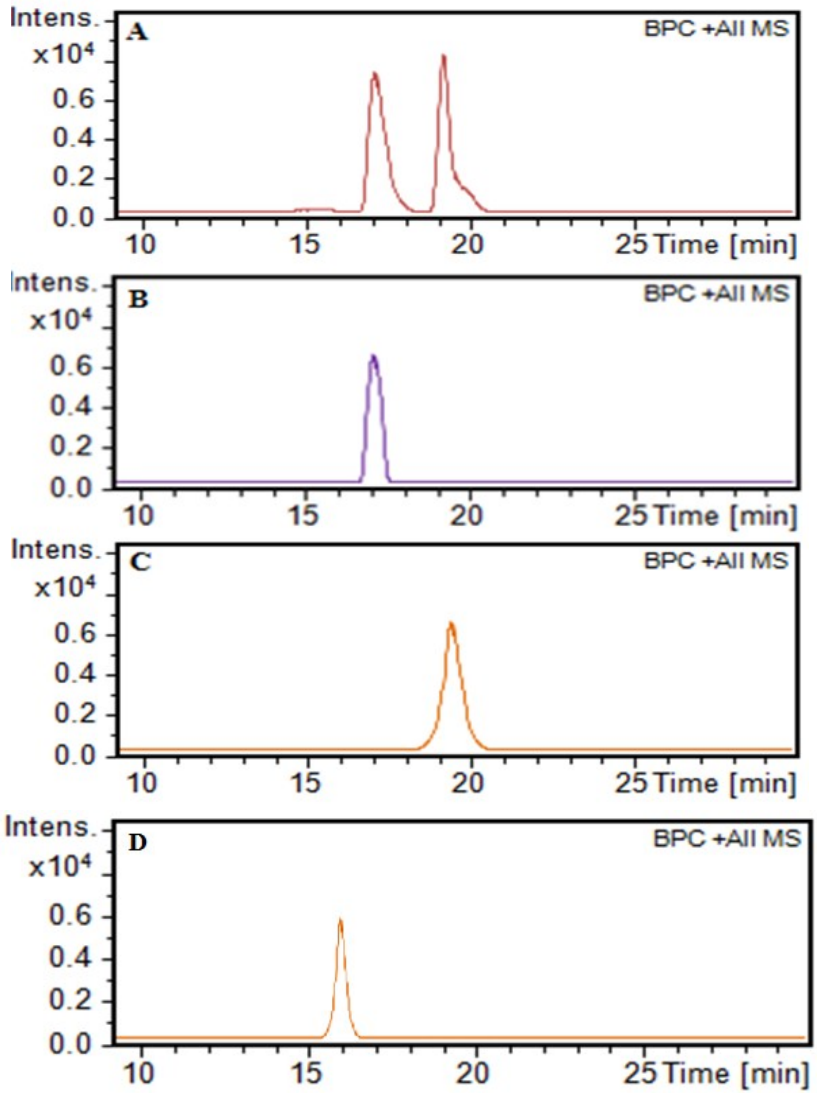

Figure S81. (A) LC chromatogram of thick oil obtained after work up of reaction mixture of compound **5d** and D-fructose. LC chromatogram of commercial samples of: (B) D-glyceraldehyde, (C) Dihydroxyacetone and (D) L-glyceraldehyde.

<u>Kinetics data for cleavage of D-fructose in presence of aldolase and compound 5d.</u>

For aldolase catalyzed reaction. Reaction mixture (2 ml) was containing fructose-1,6-bisphosphate (10^{-5} M), NADH (0.5 μM), 125 μg mixture of glycerol-1-phosphate dehydrogenase and isomerase, 500 μM Tris-HCl buffer (pH 7.4) and 50 units of aldolase

enzyme. The absorbance change at 340 nm was observed in UV spectrum with varying fructose-1,6-biphosphate conc (10^{-5} M – 10^{-4} M) and time (from 1 min – 10 min) to obtain K_m by the graph, 1/rate vs 1/conc.

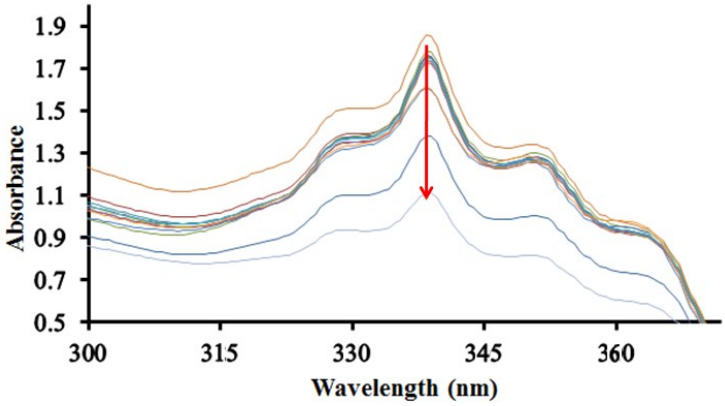

Figure S82. Change in UV spectrum of reaction mixture containing aldolase (80 units), fructose-1,6-bisphosphate (10^{-5} M), NADH (10^{-5} M) in tris-HCl buffer with increase in concentration of fructose-1,6-bisphosphate (10^{-5} – 10^{-4} M).

For compound 5d catalyzed reaction: formation of Schiff base 8. The reaction mixture was containing compound **5d** (10^{-5} M) and D-Fructose (10^{-5} M) in 2 ml DMSO:H_2O (1:9) at pH 6.0-6.5. pH of the reaction mixture was recorded at every step and maintained at 6.0-6.5 using 0.1 N HCl/0.1 N NaOH. Keeping the concentration of compound **5d** constant, the concentration of D-fructose was stepwise increased from 10^{-5} M to 10^{-4} M and the corresponding change in UV-vis spectrum at 400 nm was noted. The band at 400 nm (due to compound **5d**) underwent change as the formation of Schiff takes place (Table S1).

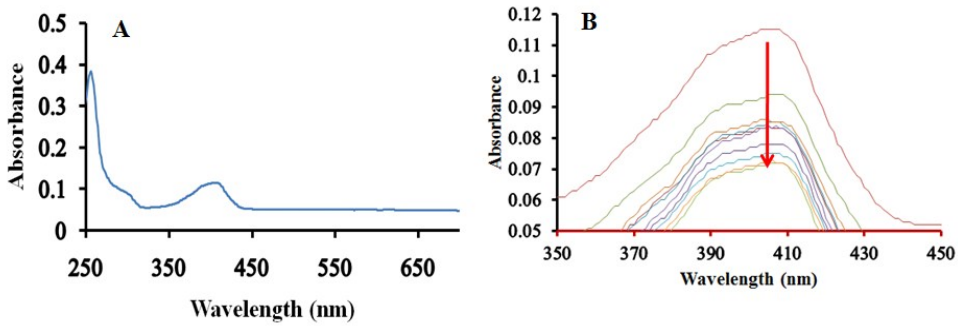

Figure S83. (A) UV-vis spectrum of compound **5d** (10^{-5} M, DMSO:H_2O, 1:9 v/v). (B) Change in UV-vis spectrum of compound **5d** at 10^{-5} M (DMSO:H_2O, 1:9) on stepwise addition of D-fructose (0 – 10 equiv, 10^{-5} M – 10^{-4} M).

Michaelis –Menton constant (K_m) was calculated from the Lineweaver-Burk equation of enzyme kinetics:

$1/V = K_m/V_{max} .1/[S] + 1/V_{max}$

V- Reaction rate (change in absorbance per unit time), K_m- Michaelis-Menton constant, V_{max}- Maximum reaction rate (change in absorbance at maximum substrate concentration per unit time), [S]- Substrate concentration.

$K_{cat} = V_{max}$ (sec^{-1})/[M], [M] is concentration of compound **5d** at V_{max}.

Table S1. Kinetics data for the formation of Schiff base **8**.

Conc of fructose (μM)	Time interval (min)	V_0 (sec^{-1}) (change in absorbance at 400 nm/time)	V_0/E_t (sec^{-1}) E_t – conc of compound **5d** (10^{-5} M)
10	1	6.66×10^{-5}	6.66
20	1	1.08×10^{-4}	10.8
30	1	1.35×10^{-4}	13.5
40	1	1.5×10^{-4}	15.0
50	1	1.75×10^{-4}	17.5
60	1	1.86×10^{-4}	18.6
70	1	1.9×10^{-4}	19.0
80	1	1.95×10^{-4}	19.5
90	1	2.01×10^{-4}	20.1
100	1	2.08×10^{-4} (V_{max})	20.8 (K_{cat})

Table S2. Catalytic efficiency of biomodels for the retroaldol reaction.

S. No.	**Reference**	**Modular assembly**	**Substrate**	**K_m (μM)**	**K_{cat} (min^{-1})**
1	*Angew. Chem. Int. Ed.* **2009**, 48, 922-925	Peptide	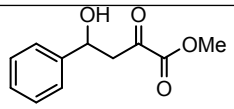	5000	0.13
2	*Chem. Commun.* **2001,** 769-770	Peptide	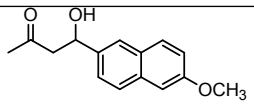	1800	2.1×10^{-4}

			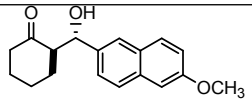	900	4.1×10^{-4}
3	*J. Am. Chem. Soc.* **2002**, 124, 3510-3511	Peptide	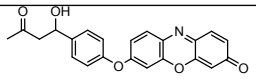	8	2.3×10^{-4}
		Peptide	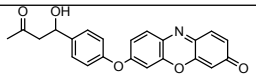	130	2.0×10^{-4}
4	*Proc. Natl. Acad. Sci USA* **1998**, 95, 15351-15355	Aldolase antibody	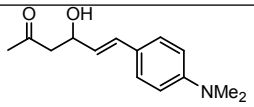	25	5.0
			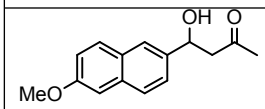	14	1.0
			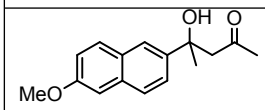	150	3.3
			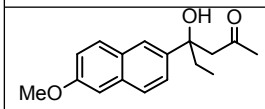	37	0.15
			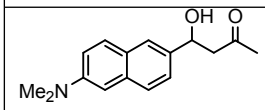	7	0.3
5	*J. Mol. Biol.* **2014**, 426, 256-271	Designed retroaldolase	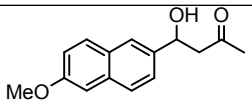	34	3.2×10^{-6}
		Designed retroaldolase	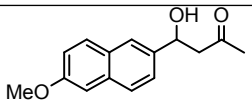	1740	1.5×10^{-5}
		Designed retroaldolase	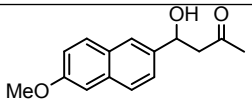	1570	1.3×10^{-5}
		Designed retroaldolase	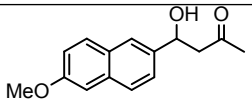	473	2.7×10^{-5}
		Designed retroaldolase	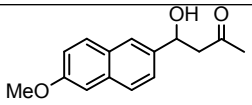	880	3.6×10^{-6}
6	**present experiments**	Aldolase	Fructose-1,6-bisphosphate	16	1620
7	**Present contribution: Compound 5d**	Tripeptide appended acridine	D-fructose	30	1248

References:

1. B. S. Furniss, A. J. Hannaford, P. W. G. Smith, A. R. Tatchell in *Vogel's Text Book of Practical Organic Chemistry*. 5th Edition. **1989**, Addison Wesley Longman Ltd. England. pp761.
2. Energy minimization was performed using PM3 basis set of software package ArgusLab4.0.1. ArgusLab 4.0.1, M. A. Thompson, Planaria Software LLC, Seattle, WA 98155.